JOC The Journal of Organic Chemistry

Featured Article

pubs.acs.org/joc

Ladder Oligo(*m*-aniline)s: Derivatives of Azaacenes with Cross-Conjugated π-Systems

Andrzej Rajca,*[,†] Przemysław J. Boratyński,[†,§] Arnon Olankitwanit,[†] Kouichi Shiraishi,[†] Maren Pink,[‡] and Suchada Rajca[†]

[†]Department of Chemistry, University of Nebraska, Lincoln, Nebraska 68588-0304, United States

[‡]IUMSC, Department of Chemistry, Indiana University, Bloomington, Indiana 47405-7102, United States

Ⓢ *Supporting Information*

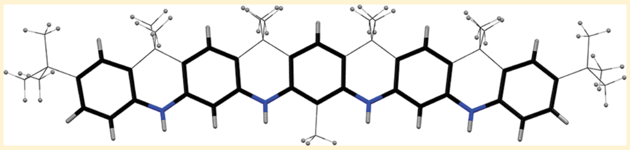

ABSTRACT: We describe the synthesis and electronic properties of ladder oligomers of poly(*m*-aniline) that may be considered as derivatives of azaacenes with cross-conjugated π-systems. Syntheses of ladder oligo(*m*-aniline)s with 9 and 13 collinearly fused six-membered rings employed Pd-catalyzed aminations and Friedel−Crafts-based ring closures. Structures were confirmed by either X-ray crystallography or correlations between DFT-computed and experimental spectroscopic data such as ^{1}H, ^{13}C, and ^{15}N NMR chemical shifts and electronic absorption spectra. All compounds have planar "azaacene" moieties. The experimental band gaps $E_g \approx 3.5-3.65$ eV, determined by the UV−vis absorption onsets, were in agreement with the TD-DFT-computed vertical excitation energies to the S_1 state. Fluorescence quantum yields of up to 20% were found. Electrochemically estimated HOMO energies of −4.8 eV suggested propensity for a facile one-electron oxidation and just sufficient environmental stability toward oxygen (O_2). For two oligomers with "tetraazanonacene" moieties, potentials of $E^{4+/3+} \approx 1.6-1.7$ V vs SCE were determined for four-electron oxidation to the corresponding tetraradical tetracations.

1. INTRODUCTION

π-Conjugated systems with ladder connectivity are of recent interest because of their potential for the development of organic materials.[1−6] Ring-fused polycyclic structures may provide superior electronic properties[2−8] as well as an opportunity to obtain molecules with well-defined, robust conformation, e.g., planar or helical.[8−21] Examples are molecules that may be viewed as fragments of graphene, or other conjugated carbon allotropes, and their heterocyclic analogues.[8−11,17−21]

Acenes are ring-fused polycyclic structures with "collinearly-fused" benzene rings, such as in pentacene, which possesses favorable p-type semiconducting properties.[22,23] The search for improved semiconducting and materials properties, as well as their interesting biradical electronic structures,[24] have driven recent synthetic effort in the preparation and studies of extended acenes with up to nine fused rings,[25,26] and acenes with solubilizing pendants.[27] This effort includes azaacenes and hydroazaacenes for development of n-type semiconductors.[28−32] In general, the extension of acene conjugated π-system beyond five fused rings faces a trade-off with lowered stability at ambient conditions.

Recently, we reported the isolation of a triplet ($S = 1$) ground-state nitroxide and aminyl diradicals, derivatives of diazapentacene (Figure 1).[33−36]

These diradicals illustrated the potential of the azaacene-based backbone as building block for high-spin aminyl polyradicals. In particular for aminyl diradical, the planar "diazapentacene" backbone demonstrated the balance between maintaining an effective $2p_\pi-2p_\pi$ overlap between the radicals, which enhances electron spin−spin interactions (exchange coupling) and provides an adequate protection for the atoms with significant spin densities that is required for isolation.[35] We plan to investigate higher homologues of the aminyl diradical derived from diazapentacene and have carried out the synthesis of ladder oligo(*m*-aniline)s **2**−**4** (Figure 2),[37] which we expect will facilitate the preparation of ladder high-spin polyradicals,[38] relevant to the design of organic magnetic materials.[8,39−42] While pursuing the synthesis of **2**−**4**, we recognized their interesting electronic structure, including that of the previously reported diamine **1**, which may be relevant to materials applications.

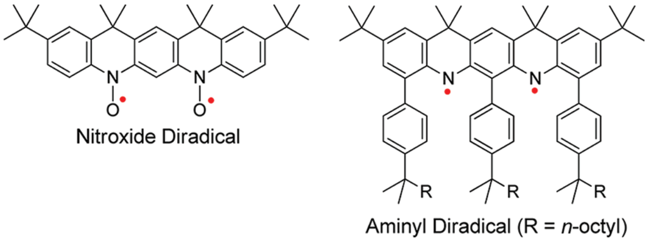

Figure 1. Triplet ground state nitroxide and aminyl diradicals with "diazapentacene" backbones.

Oligoanilines and related heterocyclic compounds with a two-dimensional ladder-like structural motif are of interest for electronic materials. The ladder polyhydro-azaborines with oligo(*m*-aniline)-like connectivity (and up to seven fused rings) have been reported. One of the polyhydro-azaborines, a

Received: December 26, 2011
Published: February 13, 2012

dx.doi.org/10.1021/jo2025948 | *J. Org. Chem.* 2012, 77, 2107−2120

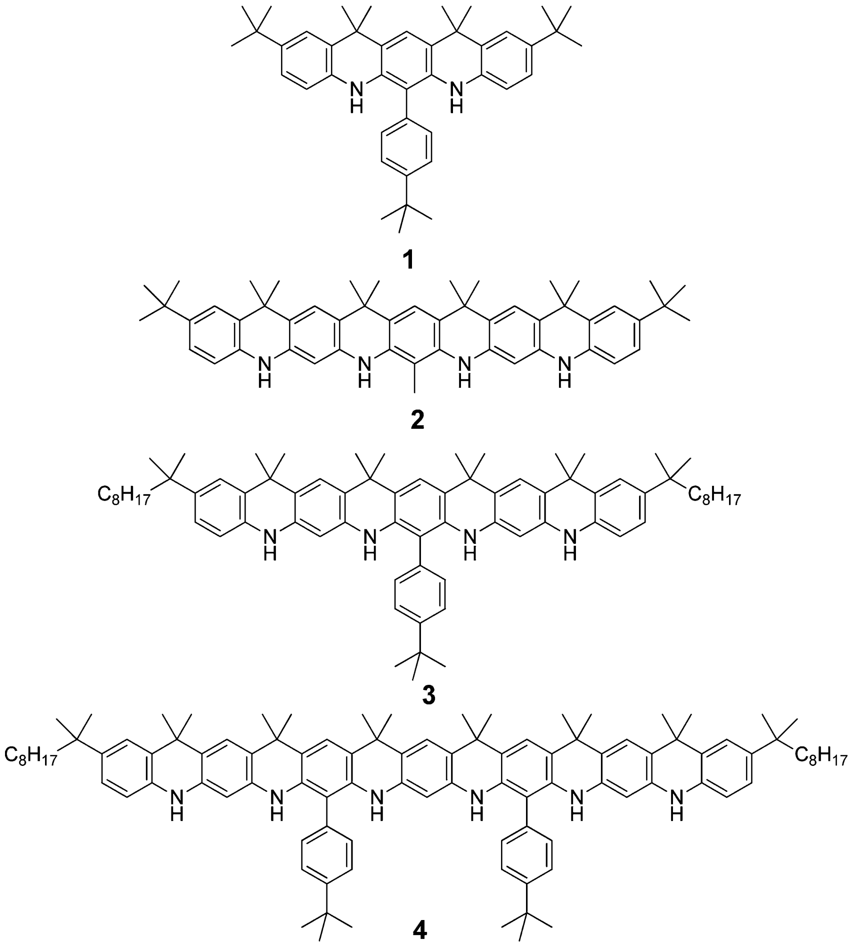

Figure 2. Ladder oligo(*m*-aniline)s: ladder oligoamines **1**−**4**.

derivative of tetrahydro-5,7-diaza-12,14-diborapentacene, possessed fluorescence quantum yields of about 98% in cyclohexane at room temperature.[43] Analogous structures with five fused rings based upon oxygen−nitrogen- and sulfur−nitrogen-containing heterocycles have been studied as hole injection materials in light-emitting diodes. For example, emitting devices constructed from 5,7,12,14-tetrahydro-5,7-bis(1-naphthyl)-5,7-diaza-12,14-dithiopentacene showed a long half-life of 90 h at high current densities (50 mA/cm^2) and a high emitting efficiency (2.6 lm/W).[44] The ladder oligo(*p*-aniline) structures containing indolocarbazole units with up to nine fused rings have been synthesized,[45] and an oligomer with five fused rings was reported to provide semiconductors for p-type field-effect transistors with promising mobilities (0.2 cm^2 V^{-1} s^{-1}) and on/off current ratios (>10^6).[46]

From another point of view, we consider oligo(*m*-aniline)s **1**−**4** as derivatives of azaacenes (hydroazaacenes) with cross-conjugated π-systems.[47] The corresponding hydroazaacene backbones, tetrahydrodiazapentacene, octahydrotetraazanonacene, and dodecahydrohexaazatridecacene, with up to 13 fused rings, are illustrated in Figure 3. Cross-conjugation is expected to improve environmental stability of hydroazaacenes and result in a larger band gap with increased transparency in the visible region, compared to acenes.[19,48,49] Cross-conjugated π-systems are being explored for electron transport in molecular junctions, optical materials, and sensors.[50,51]

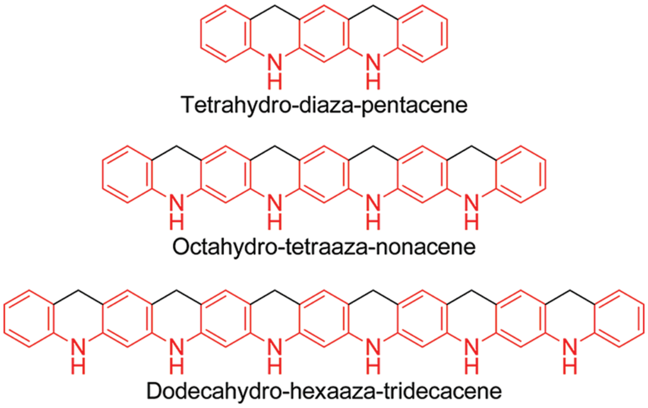

Figure 3. Ladder oligo(*m*-aniline)s: hydroazaacenes with cross-conjugated π-systems.

We report efficient syntheses of the extended derivatives of hydroazacenes, ladder oligoamines **2**−**4** with up to 13 collinearly fused six-membered rings (Figure 2). Ladder oligoamines **1**−**4** were characterized by UV−vis absorption and fluorescence spectroscopy and voltammetry. Both experiments and computations (DFT and TD-DFT) indicate that within the series of **1**, **3**, and **4**, HOMO energies and band gaps show negligible change between tetraamine **3** and hexamine **4**.

2. RESULTS AND DISCUSSION

2.1. Synthesis of Ladder Tetraamine 2. Our synthetic route to ladder tetraamine **2** is based upon the palladium-catalyzed C−N coupling reactions (aminations), followed by annelation forming six-membered rings (Scheme 1). In the first step, amination of 4,6-diisopropenyl-1,3-dibromobenzene[36] with 4-*tert*-butylaniline using $\mathrm{Pd(OAc)_2}$/1,1′-bis(diphenylphosphino)ferrocene (DPPF) as catalyst[52] provides monoamine **6**. In the subsequent C−N coupling reactions of **6** with 2,6-diaminotoluene and 1,3-diaminobenzene, a more reactive catalyst such as $\mathrm{Pd(OAc)_2/P(}t\mathrm{\text{-}Bu)_3}$ is used[37a,53,54] to provide tetraamines **7** and **8**, respectively. Quadruple ring closure of **7** in 85% phosphoric acid, via Friedel−Crafts-type electrophilic aromatic substitution,[33a,36,55] gives ladder tetraamine **2** with nine collinearly fused rings in very good yields (90−95% per ring closure); from the analogous reaction of **8** in phosphoric acid (or 1:1 phosphoric/sulfuric acid mixture), only an "angular" tetraamine **5** is isolated in low yields.[56] These results suggest that the "blocking" group, such as methyl group in **2**, is essential for the synthesis of collinearly fused oligo(*m*-anilines).

Scheme 1. Synthesis of Ladder Tetraamines 2 and 5

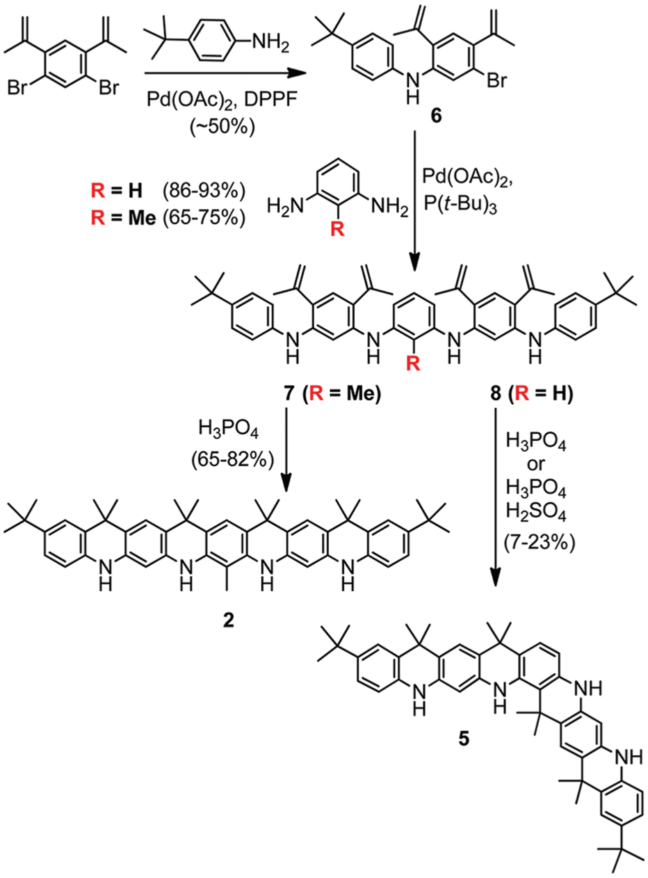

2.2. Synthesis of Ladder Tetraamine 3 and Hexaamine 4. Because the ladder tetraamine **2** (and **5**) is poorly soluble in common organic solvents, we sought to modify the synthesis by introducing solubilizing groups, such as 4-*tert*-butyl-phenyl pendants[34] and *tert*-undecyl chains.[35] This can be accomplished by the preparation of building blocks **11** and **14**, which are analogous to **6** and 2,6-diaminotoluene in the synthesis of **2**. As shown in Scheme 2, building block **11** and **14** are prepared from 2-methyl-2-phenyldecane[35] and 1,3-dibromo-2-iodobenzene.[57]

The C−N coupling reaction of **11** with **14** in a 2.2:1 molar ratio gives tetraamine **15** in 45−62% isolated yields (Scheme 3). Hexaamine **17**, is obtained via two consecutive C−N coupling reactions: (1) **11** and **14** in the 1:1 molar ratio provide triamine **16** in 34−43% isolated yields and (2) triamine **16** and 4,6-diisopropenyl-1,3-dibromobenzene in a 2:1 molar ratio give **17** in 41−48% isolated yields.

Scheme 2. Synthesis of Building Blocks 11 and 14 for Tetraamine 3 and Hexaamine 4

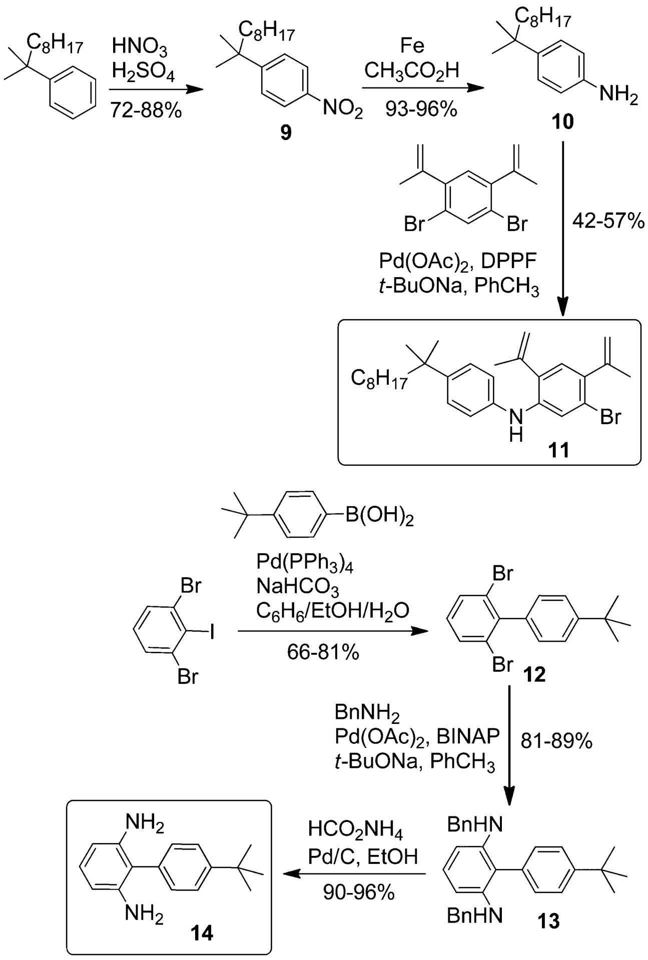

Ladder tetraamine **3** and hexaamine **4** are obtained from **15** and **17**, respectively, by Friedel−Crafts-type ring closures in a 1:1 mixture of 85% phosphoric acid and 98% sulfuric acid at 55−60 °C for about 15 min under nitrogen atmosphere. ^{1}H NMR spectra of selected crude reaction mixtures indicate excellent yields for **3** and **4**, specifically almost quantitative yields for **3** (Figures S77, S78, and S83, Supporting Information). Even though small amounts of starting material and byproduct are observed in some other crude reaction mixtures, this result indicates an extraordinary efficiency for the closures of four and six rings in **3** and **4**, respectively. Purification of the crude reaction mixtures by flash chromatography at 0 °C on silica deactivated with triethylamine provides a range of isolated yields of **3** and **4** (Scheme 3), perhaps due to the sensitivity of the ladder oligoamines to acidic environments such as silica, even after deactivation with triethylamine.[58] In the case of **4**, another complicating factor in chromatographic purification is its modest solubility in typical organic solvents.

2.3. Structure of Ladder Oligoamines. *X-ray Structure of* **2**. The structure of tetraamine **2** is established by X-ray crystallography using synchrotron radiation (Figure 4). The nine collinearly fused six-membered rings form an approximately planar π-system; the mean deviation from a calculated least-squares plane (C1−C34, N1−N4) is 0.0559 Å, which may

Scheme 3. Synthesis of Tetraamine 3 and Hexaamine 4

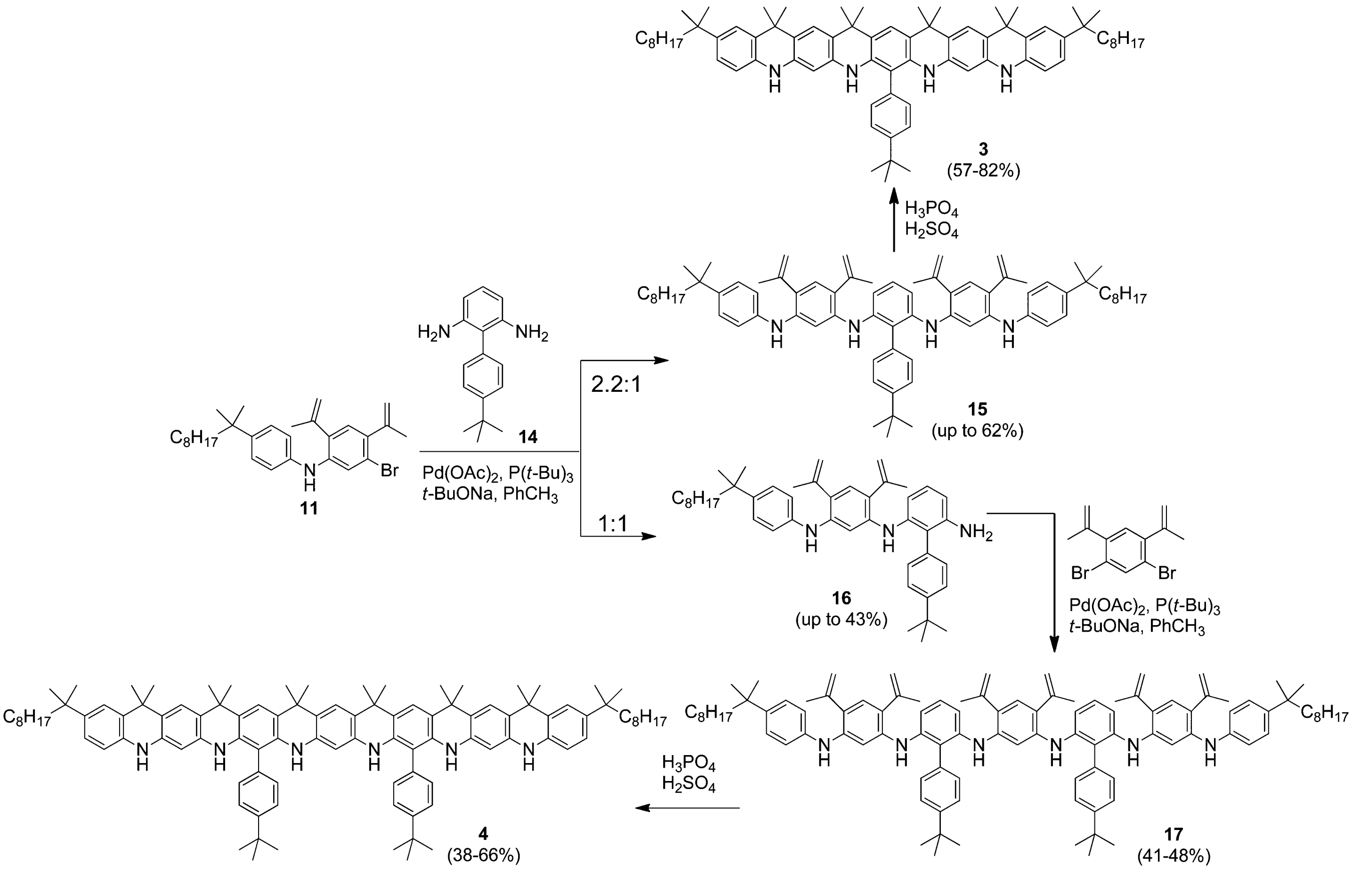

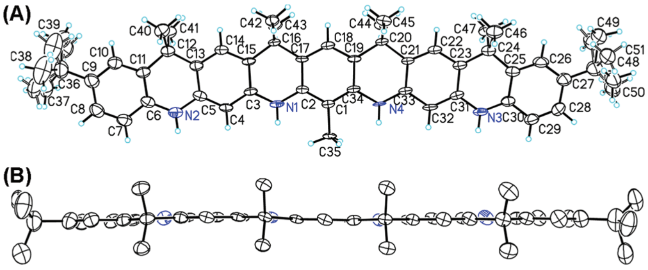

Figure 4. Molecular structure and conformation for **2**: (A) top view of **2**; (B) side view of **2**. Carbon and nitrogen atoms are depicted with thermal ellipsoids set at the 50% probability level; disorder is omitted for clarity. In the side view, hydrogen atoms are omitted. Further details are reported in Table S1 and Figures S1−S3, Supporting Information.

be compared to the mean deviation of 0.0763 Å found for the analogous plane of five collinearly fused six-membered rings in diamine **1**.[34] The computed structure of **2** at the B3LYP/6-31G(d,p) level also provides a similar planar geometry, though the out-of-plane vibrational mode with the lowest frequency is in the range of about 10 cm^{-1} (Table S4, Supporting Information), indicating considerable flexibility for the "tetraazanonacene" moiety.

Interestingly, tetraamine **2** shows in-plane bending of the ladder structure. This bending may be associated with the presence of *gem*-dimethyl ($\mathrm{C(Me)_2}$) bridges with eight $\mathrm{C(sp^3)}$−$\mathrm{C(sp^2)}$ bonds of about 1.5 Å that are longer than $\mathrm{C(sp^2)}$−$\mathrm{C(sp^2)}$ and C−N bond lengths of about 1.4 Å (for further analyses, see Figure 6 and Table 2).

*Determination of Structures **3** and **4** Using NMR Spectroscopy and DFT-Computed NMR Chemical Shifts.* The structures of tetraamine **3** and hexaamine **4** are confirmed by the assignment of their experimental ^{1}H and ^{13}C NMR spectra in acetone-d_6 or benzene-d_6 using standard 2D NMR spectroscopy, including ^{1}H−^{13}C HSQC, long-range ^{1}H−^{13}C HMBC, ^{1}H−^{1}H NOESY, and ^{1}H−^{15}N HSQC (Figures S36−S47, Supporting Information).[59] Diamine **1**, for which the X-ray structure has been reported,[34] is subjected to similar NMR experiments and serves as a reference for **3** and **4**.

Additional evidence in support of ladder structures **3** and **4** is obtained from the correlation between the DFT-calculated and experimental ^{1}H and ^{13}C NMR chemical shifts. Diamine **1**, as well as the simplified structures **3a** and **4a** corresponding to **3** and **4**, in which the *tert*-undecyl groups are replaced with *tert*-butyl groups, are studied (Figure 5). Geometries of **1**, **3a**, **4a**, and tetramethylsilane were optimized at the B3LYP/6-31G(d,p) level of theory and confirmed as minima by vibrational analyses.[60] In all structures, the "azaacene" moieties are planar, similar to that found in the X-ray structures of **1**[34] and **2** (Figure 4). Also, the dihedral angle of 75.82(4)° between the planes of the azaacene moiety and the *tert*-butylphenyl pendant in the X-ray structure of **1** is in good agreement with the corresponding torsion angles of about 75.1° in the DFT-optimized geometry of **1**.

Using these DFT-optimized geometries, ^{1}H and ^{13}C NMR isotropic shieldings for **1**, **3a**, **4a**, and tetramethylsilane are computed at the GIAO/B3LYP/6-31G(d,p) level of theory with the IEF-PCM-UA0 solvent model for acetone or benzene (Gaussian 03),[60−62] to provide calculated ^{1}H and ^{13}C NMR chemical shifts $\delta_{\mathrm{DFT}}(^{1}\mathrm{H})$ and $\delta_{\mathrm{DFT}}(^{13}\mathrm{C})$ for direct comparison with the experimental NMR spectra of **1** and **3** in acetone-d_6 and **4** in benzene-d_6.[33c] The correlations between DFT-computed and experimental ^{13}C NMR chemical shifts give correlation coefficients (R^2) that are expected for correctly assigned

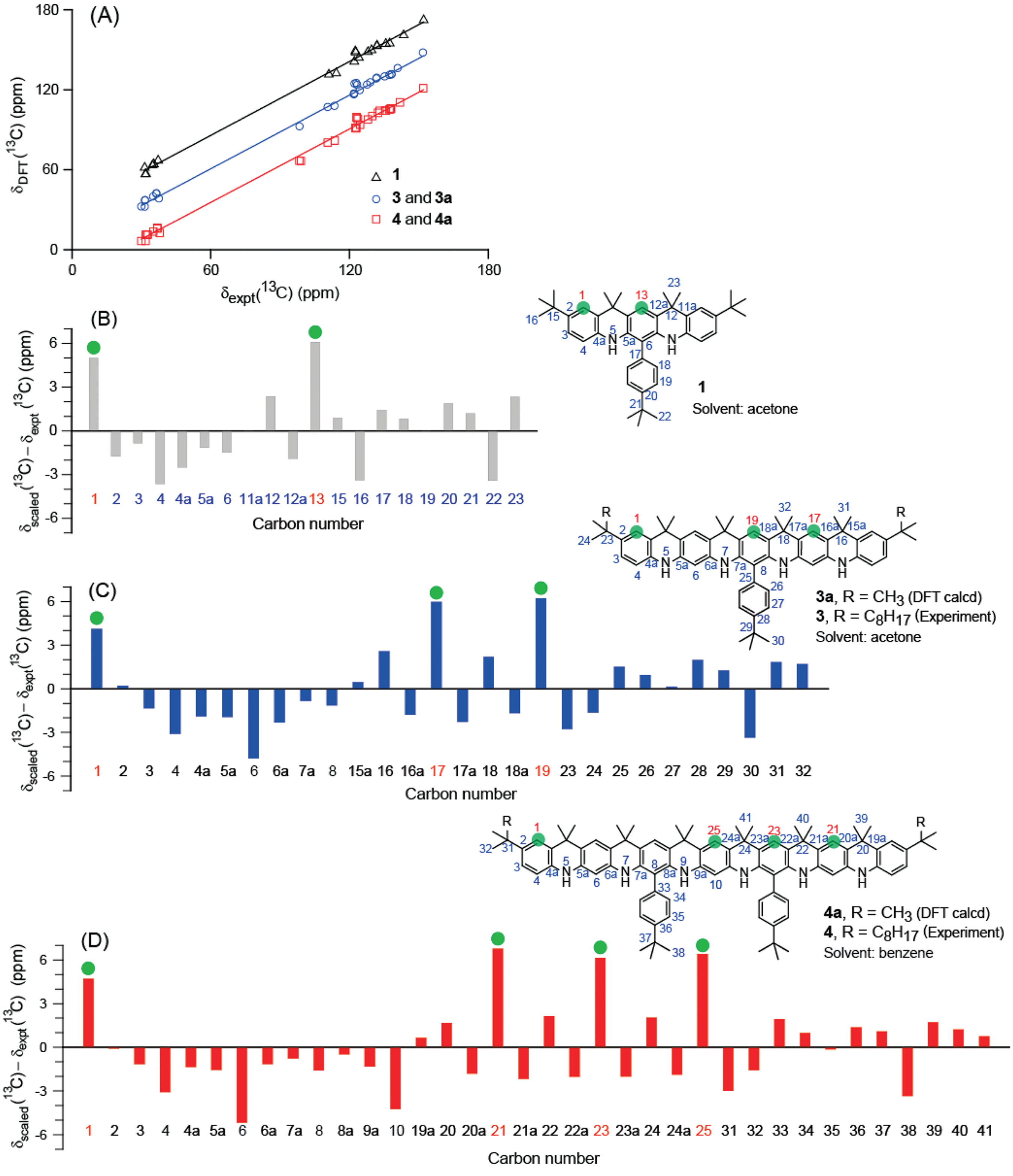

Figure 5. (A) Correlations between calculated (δ_{DFT}) and experimental (δ_{expt}) ^{13}C NMR chemical shifts for **1**, **3a**, **4a** and **1**, **3**, **4**, respectively. Solid lines are the best fit to $\delta_{\mathrm{DFT}} = a + b\ \delta_{\mathrm{expt}}$. (B–D) Difference between scaled ($\delta_{\mathrm{scaled}} = (\delta_{\mathrm{DFT}} - a)/b$) and experimental ($\delta_{\mathrm{expt}}$) ^{13}C NMR chemical shifts; highlighted differences correspond to carbon atoms on the "outer rim" of the azaacene moieties. Statistical parameters are summarized in Table 1. Further details are reported in Table S6, Supporting Information.

structures of medium sized organic molecules (Figure 5A and Table 1).[62,63]

The relationship between computed and experimental NMR chemical shifts is further illustrated by applying the correlations to scale linearly $\delta_{\mathrm{DFT}}(^{13}\mathrm{C})$, to provide $\delta_{\mathrm{scaled}}(^{13}\mathrm{C})$, and then by plots of the differences between the scaled and experimental NMR chemical shifts for each distinct carbon atom in the structure (Figures 5B–D).[33c,62] These plots confirm the good agreement between the theory and experiment, and specifically the low values of statistical parameters for ^{13}C NMR chemical

Table 1. Statistical Parameters for the Correlations of ^{13}C and ^{1}H NMR Chemical Shifts[a]

	a	*b*	R^2	MaxErr	CMAE
1 (^{13}C)	5.317	0.9230	0.9966	6.08	2.106
3/3a (^{13}C)	5.404	0.9204	0.9962	6.22	2.211
4/4a (^{13}C)	5.339	0.9178	0.9957	6.77	2.206
1 (^{1}H)	−0.026	1.0212	0.9966	0.40	0.112
3/3a (^{1}H)	−0.072	1.0206	0.9912	0.73	0.169
4/4a (^{1}H)	−0.075	1.0125	0.9942	0.39	0.172

[a] *a* and *b* are the intercept and slope of the linear fit to $\delta_{\mathrm{DFT}} = a + b\,\delta_{\mathrm{expt}}$, and R^2 is its correlation coefficient. MaxErr is the maximum corrected absolute error with respect to the linear fit ($|\delta_{\mathrm{scaled}} - \delta_{\mathrm{expt}}|$). CMAE is the corrected mean absolute error for *n* chemical shifts ($(\sum|\delta_{\mathrm{scaled}} - \delta_{\mathrm{expt}}|/n)$).

shifts such as MaxErr and CMAE in Table 1, as expected for correctly assigned structures. Furthermore, the plots reveal the presence of similar systematic errors in the structures of diamine, tetraamine, and hexaamine. For example, ^{13}C NMR chemical shifts for carbon atoms on the "outer rim" of the azaacene moieties are consistently overestimated by DFT by about 4−7 ppm (chemical shift differences highlighted in Figures 5B−D). Because the structure of diamine **1** was established by X-ray crystallography, the ^{13}C NMR chemical shift correlations that include **1** confirm structures of the higher homologues **3** and **4**.

Similar analyses of the relationship between computed and experimental ^{1}H NMR chemical shifts are summarized in Table 1 and illustrated in the Supporting Information (Figures S27−S32). As the IEF-PCM solvent model does not properly account for specific solvent−solute interactions such as hydrogen bonding,[64] the protons of NH moieties are not included in the analyses. As DFT computations of ^{1}H NMR chemical shifts tend to be less accurate, overall agreement between theory and experiment is less satisfactory for ^{1}H, compared to ^{13}C NMR chemical shifts.[33c,61]

^{1}H−^{15}N HSQC spectra for **1**, **3**, and **4** show the expected number of cross-peaks between ^{1}H and ^{15}N confirming the presence of one, two, and three nonequivalent NH groups, respectively (Figures S33, S36, and S42, Supporting Information). The ^{15}N NMR chemical shifts are clustered around $\delta = -286$ ppm (relative to nitromethane at 0.0 ppm), which is within the typical range for NH groups in amines; also, DFT-calculated ^{15}N NMR chemical shifts for these NH groups are within 2 ppm of the experimental values (Table S7, Supporting Information).

For angularly annelated ladder tetraamine **5**, characterization by NMR spectroscopy was hindered by its air-sensitivity, poor solubility, and limited availability. ^{1}H NMR spectra (1D and 2D COSY) of **5** indicate the presence of two AMX (or ABX) spin coupling systems for 4-*tert*-butyl-substituted benzene rings and AX (or AB) set of doublets for the center benzene ring; the other two benzene rings appear as four 1-proton singlets. Another set of four H/D exchangeable 1-proton singlets are assigned to the NH groups. In the aliphatic region, two distinct *gem*-dimethyl moieties with diastereotopic methyl groups (4 different methyl groups) and two distinct *tert*-butyl groups are found.

Bent Ladder Geometry. As illustrated by the X-ray structure of tetraamine **2** (Figure 2), analogous ladder oligoamines with C(Me$_2$) bridges are expected to show in-plane bending of the ladder. For each bent ladder oligoamine, the carbon and nitrogen atoms at the inner rim may be viewed as forming an arc, a part of circumference of a circle, as illustrated for the DFT-computed structure of octaamine **18** in Figure 6. Specifically, the circle is defined by the radius, $R = d/(2\sin(180 - \alpha))$, where *d* is the distance between terminal carbon atoms of the inner rim (or chord of the circle) and α is the segment CCC angle defined in Figure 6.

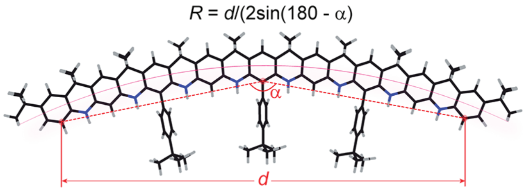

Figure 6. B3LYP/6-31G(d,p) geometry of octaamine **18** and definition of radius (*R*) for "bent" ladder.

Analyses of DFT-optimized geometries for homologous di-, tetra-, hexa-, and octaamines, as well as X-ray structures of **1** and **2**, suggest that the bending of the ladder corresponds to a circle radius of 50−60 Å (Table 2). A complete circle would require about 130 fused rings, corresponding to hexaamine **4** extended 10 times.

Table 2. "Bent" Ladder Geometry of X-Ray Structures and DFT-Optimized Geometries at the B3LYP/6-31G(d,p) Level

	d (Å)		α (deg)		*R* (Å)	
compd	X-ray	DFT	X-ray	DFT	X-ray	DFT
1	9.617	9.627	174.93	175.6	54.4	62.3
2	19.185	19.13	171.11	168.7	62.1	47.1
3a		19.14		169.5		52.3
4a		28.48		163.4		50.0
18		37.58		158.3		50.9

These results are consistent with the radii obtained for the outer rims of the ladders. For tetra-, hexa- and octaamines, radii for the outer rim corrected for the rim-to-rim distance have the values within 2 Å of the corresponding radii for the inner rim in Table 2; diamine **1** shows larger deviations of about 5 Å.

2.4. Electronic Structure of Oligoamines 1−4.

UV−vis Absorption and Fluorescence Spectroscopy. Absorption spectra for **1**−**4** in cyclohexane show similar spectral envelopes with $\lambda_{\max} = 275{-}278$ nm and $\varepsilon_{\max}$ increasing with the number of diarylamine moieties (Figure 7). Onsets of absorption (λ_{onset}), determined by the tangent method (Figure S9, Supporting Information), are dependent both on the length of the ladder and the pendant group (methyl vs 4-*tert*-butylphenyl); values of λ_{onset} appear to saturate for **3** and **4**, the cross-conjugated oligo(*m*-aniline)s ladders with 4-*tert*-butylphenyl pendants (Table 3). The band gap, $E_g \approx 3.5$ eV, is estimated for such ladder oligomers.

Fluorescence spectra of **1**, **3**, and **4** are nearly identical, showing featureless bands with $\lambda_{\max} \approx 400$ nm and large Stokes shifts of over 120 nm. Quantum yields of fluorescence, ϕ_f, are on the order of 1% only. These findings suggest that the emitting excited state has a relatively low energy and possesses geometry that is significantly different from the ground state. Most likely, torsional angles of the biphenyl moieties are decreased in the excited state. Such fluorescence properties and changes in geometry of excited states are well-known for biphenyls, including *N*,*N*-diethyl-2-aminobiphenyl.[65]

For comparison, the fluorescence band of **2** with pendant methyl group shows vibrational structure and considerably smaller Stokes shift (~80 nm). The fluorescence quantum yield, $\phi_f = 23\%$, is significantly increased. The intersection between the normalized fluorescence spectrum and either normalized

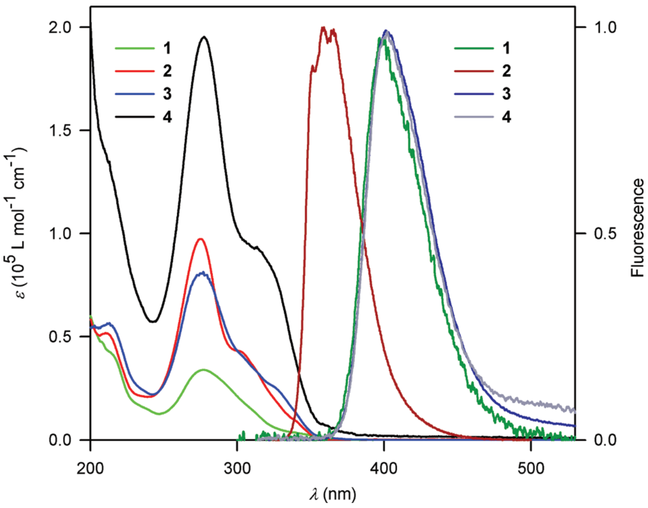

Figure 7. UV−vis electronic absorption and fluorescence spectra for ladder diamine **1**, tetraamines **2** and **3**, and hexaamine **4** in cyclohexane. Spectral parameters are summarized in Table 3. Excitation spectra are plotted in Figures S5−S8, Supporting Information.

absorption or excitation spectrum is at a wavelength of 340 nm, the same as the onset of absorption, corresponding to E_g = 3.65 eV.

The band gaps of ~3.5 and 3.65 eV may be compared to the experimental excitation energies of 4.00 and 3.31 eV for naphthalene and anthracene.[66]

Electrochemistry. Cyclic voltammograms indicate reversible oxidations in the 0.5−1.1 V range corresponding to the removal of up to two electrons for **1**, three electrons for **2** and **3**, and four electrons for **4** (Figure 8). The first oxidation potentials $E^{1+/0}$ (and onsets of oxidation) are similar for **1−4**, $E^{1+/0} \approx$ 0.6 V for **1** and 0.5 V for **2** − **4** (Table 4), because it is expected that the aminium radical cations formed by one-electron oxidation of cross-conjugated oligoamines will be localized on a single diarylaminium moiety. Such charge/spin localization was reported in the isoelectronic radical anions formed by oxidation of cross-conjugated carbopolyanions.[67] The first oxidation potentials $E^{1+/0} \approx$ +0.5 V (vs SCE) of oligoamines **2−4** is low enough for facile oxidation and just high enough for environmental stability at ambient conditions with respect to oxidation by O_2.[68]

The onsets of oxidation suggest that the HOMO energy is about −4.9 eV in diamine **1** and −4.8 eV in the tetraamines and the hexaamine (Table 4).[69,70] These energies are similar to those found in EDOT/benzo[*c*]thiophene terthiophene[71] [EDOT = 3,4-ethylenedioxythiophene] and they are higher than −5.1 eV for pentacene.[27b]

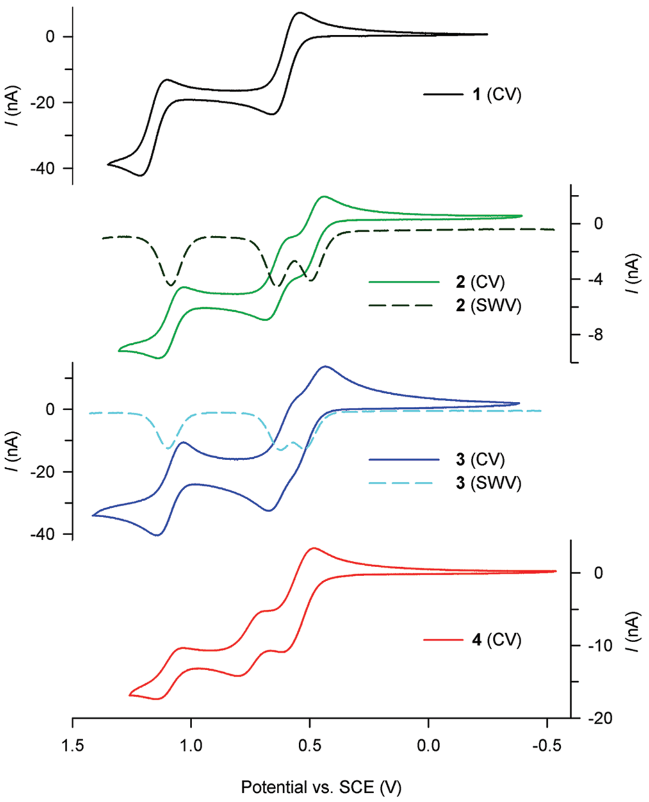

Figure 8. Cyclic voltammograms (CV, 50 mV s^{-1}) and square wave voltammograms (SWV, frequency 10 Hz, pulse height 25 mV) for ladder diamine **1**, tetraamines **2** and **3**, and hexaamine **4** in 0.1 M $[n\text{-}Bu_4N]^+[PF_6]^-$ in dichloromethane, and internally referenced to $Cp^*_2Fe^{+/0}$ (−0.130 V vs SCE).[73] Voltammograms including decamethylferrocene reference are shown in Figures S10−S16, Supporting Information. Oxidation potentials are summarized in Table 4.

The potential separation between the first two one-electron oxidations decreases from 0.56 V in diamine **1**, to 0.10−0.14 V in tetraamines **2** and **3**, and it becomes unresolvable in hexaamine **4**. The subsequent one-electron oxidations in **2−4** become more difficult with potentials increasing in 0.4−0.5 V increments. For example, the fourth oxidation potentials of **2** and **3**, corresponding to the formation of tetraradical tetracations, are much more positive, $E^{4+/3+} \approx$ 1.6−1.7 V (Table 4), and could be measured with square wave voltammetry (Figures S17 and S18, Supporting Information).[72] These trends in oxidation potentials may be ascribed to stronger and weaker repulsive electrostatic interactions between aminium radical cations localized on the nearest neighbor and non-nearest neighbor diarylaminium moieties, respectively. For example, in the diradical dication of **2**, two aminium radical cations may be

Table 3. Optical Properties for Ladder Oligoamines 1−4[a]

	absorption					fluorescence			
	λ_{max} (nm)	ε_{max} (10^4 L mol^{-1} cm^{-1})	λ_{onset} (nm)	band gap E_g[a] (eV)	excitation spectrum λ_{max}[b] (nm)	λ_{exc} (nm)	λ_{max} (nm)	ϕ_f[c] (%)	Stokes shift[d] (nm)
1	277	4.2	333	3.72	274	283	397	1.4	123
2	275, 300 (sh)	9.7, 4.3 (sh)	340	3.65	276	275, 300	351, 358, 365	23	~80
3	276	8.6	352.5	3.52	274	275, 320	401	1.6	127
4	278	19.7	351.5	3.53	275	277, 313	399	1.0	124

[a] Band gap estimated form the onset of absorption (λ_{onset}). [b] Excitation spectra observed at the fluorescence maximum (Figures S5−S8 Supporting Information). [c] Fluorescence quantum yield in cyclohexane calculated with quinine sulfate as standard; average from two excitation wavelengths for **2−4**. [d] Stokes shift estimated from excitation and fluorescence spectra λ_{max}.

Table 4. Oxidation Potentials for Ladder Oligoamines 1–4[a]

compd	oxidation potentials	CV $E_{1/2}^{ox}$ (V)	SWV E_p^{ox} (V)	CV E_{HOMO}[b] (eV)
1	$E^{+/0}$	0.601 ± 0.004	0.600 ± 0.004	−4.9
	$E^{2+/+}$	1.158 ± 0.004	1.160 ± 0.004	
2	$E^{+/0}$	0.494 ± 0.014	0.496 ± 0.002	−4.8
	$E^{2+/+}$	0.628 ± 0.014	0.638 ± 0.002	
	$E^{3+/2+}$	1.087 ± 0.014	1.084 ± 0.004	
	$E^{4+/3+}$		1.663 ± 0.002	
3	$E^{+/0}$	0.516 ± 0.008	0.525 ± 0.008	−4.8
	$E^{2+/+}$	0.612 ± 0.002	0.622 ± 0.004	
	$E^{3+/2+}$	1.092 ± 0.004	1.098 ± 0.006	
	$E^{4+/3+}$		1.654 ± 0.026	
4	$E^{2+/0}$	0.544 ± 0.006		−4.8
	$E^{3+/2+}$	0.743 ± 0.020		
	$E^{4+/3+}$	1.092 ± 0.016		

[a] Potentials (vs SCE) from cyclic voltammetry (CV) and square wave voltammetry (SWV) based on average values from multiple voltammograms with scan rates of 20–500 or 50–500 mV s^{-1} (and with frequency of 10 Hz) in 0.1 M $[n\text{-}Bu_4N]^+[PF_6]^-$ in dichloromethane; 100 μm Pt-disk as working electrode. The potentials are calibrated with decamethylferrocene as the internal standard (−0.130 V vs SCE for $Cp^*{}_2Fe^{+/0}$ in dichloromethane).[73] [b] Calculated using the empirical relationship $E_{HOMO} = -(E^{ox}_{onset} + 4.4)$;[69,70] further details in Figures S10–S16, Supporting Information.

localized on non-nearest neighbor diarylaminium moieties, however, in the triradical trication one strong repulsive interaction to the nearest neighbor diarylaminium moieties is added, and in tetraradical tetracation two more such interactions are added.

Square wave voltammograms of **2** and **3** (and cyclic voltammograms) show that the onsets of reduction of tetraamines are at potentials that are more negative than about −2.2 V (vs SCE), which is approximately the potential limit for our supporting electrolyte, $[n\text{-}Bu_4N]^+[PF_6]^-$ in dichloromethane, and Pt-electrode (Figures S19–S22, Supporting Information).[72] Because onsets of oxidation are at about +0.4 V (vs SCE), these results indicate that the band gap $E_g > 2.6$ V, in qualitative agreement with $E_g = 3.65$ eV and $E_g = 3.52$ eV obtained from optical data for **2** and **3**, respectively.

Computed Band Gaps. DFT energies of frontier MOs and time-dependent DFT (TD-DFT) vertical excitations were calculated at the B3LYP/6-31G(d,p) level of theory with the IEF-PCM-UA0 solvent model for cyclohexane using B3LYP/6-31G(d,p)-optimized geometries in the gas phase.[60]

DFT energies of HOMOs for **1**, **2**, **3a**, and **4a** show a similar trend for the experimental values of HOMOs for **1–4** obtained from electrochemical experiments, though computations using a relatively small double-ξ basis set overestimate the experimental values in dichloromethane by 0.4–0.5 eV (Table 5). The computed energy of the LUMO is about 0.3 eV higher for methyl-substituted tetraamine **2** and unsubstituted derivatives **19** and **20** (Chart 1) than that for 4-*tert*-butylphenyl-substituted **1**, **3a**, and **4a**; consequently, the HOMO–LUMO gap (Δε) for **2** (as well as **19** and **20**) is correspondingly higher than the "converged" Δε ≈ 4 eV for **3a**, **4a**, and "homologous" octaamine **18**. These Δε overestimate experimental band gaps (E_g) by about 0.5 eV for **1**, **3**, and **4** and by 0.7–0.8 eV for **2**.

Chart 1. Structures of Diamine 19 and Tetraamine 20

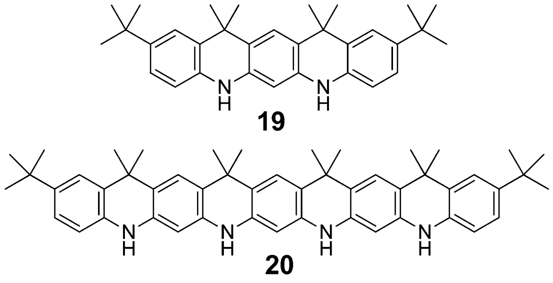

TD-DFT computed UV–vis spectra for **1**, **2**, **3a**, and **4a** are in agreement with the experimental spectra for **1–4**; slight red-shift for the Gaussian envelope of the TD-DFT spectra obtained with B3LYP functional is observed (Figure 9).[74,75] In contrast to Δε, TD-DFT computed vertical excitation energies to the lowest excited state ($\Delta E(S_0-S_1)$) reproduce the experimental E_g quite well.[75] Specifically, values of $\Delta E(S_0-S_1)$ are within about 0.2 eV of experimental E_g for **1** and **2**; for **3a** and **4a**, values of $\Delta E(S_0-S_1)$ are nearly coincident with E_g for **3** and **4**. Values of $\Delta E(S_0-S_1)$ for **2**, **19**, and **20** are within 0.02 eV, suggesting that the effect of the methyl group in **2** on the band gap is very small (Table 5).

3. CONCLUSION

Ladder oligomers of poly(*m*-aniline), with up to 13 collinearly fused six-membered rings were prepared by Pd-catalyzed aminations and Friedel–Crafts-based ring closures. Such oligomers may be considered as derivatives of hydroazaacenes with cross-conjugated π-systems. The experimental $E_g \approx 3.5$ eV for tetraamine **3** and hexaamine **4** (with 4-*tert*-butylphenyl pendants), determined by the UV–vis absorption onsets, is in excellent agreement with the TD-DFT-computed vertical excitation energies to the S_1 state (3.5 eV) for the analogous model tetraamine and hexaamine. In comparison, the experimental E_g for tetraamine **2** (with methyl pendant) is somewhat higher, $E_g \approx 3.65$ eV, with a TD-DFT excitation energy of 3.87 eV. Among the ladder oligoamines **1–4** (Figure 2), the optical

Table 5. Energies of Frontier Molecular Orbitals (ε_{HOMO} and ε_{LUMO}), HOMO–LUMO Gaps (Δε), and Vertical Excitation Energies to the S_1 State ($\Delta E(S_0-S_1)$, in eV) for Ladder Oligoamines in Cyclohexane[a]

compd	ε_{HOMO}	ε_{HOMO} (expt)	ε_{LUMO}	Δε	$\Delta E(S_0-S_1)$	E_g (expt)
diamine **1**	−4.537 (−4.496)	−4.9	−0.371 (−0.425)	4.17 (4.07)	3.56	3.72
tetraamine **2**	−4.489 (−4.489)	−4.8	−0.082 (−0.079)	4.41 (4.41)	3.87	3.65
tetraamine **3a**	−4.450 (−4.424)	−4.8	−0.388 (−0.460)	4.06 (3.96)	3.50	3.52
hexaamine **4a**	−4.411 (−4.364)	−4.8	−0.387 (−0.454)	4.02 (3.91)	3.49	3.53
octaamine **18**	−4.394 (−4.337)		−0.412 (−0.471)	3.98 (3.87)	3.46	
diamine **19**	−4.561 (−4.582)		−0.059 (−0.069)	4.50 (4.51)	3.88	
tetraamine **20**	−4.466 (−4.490)		−0.068 (−0.081)	4.40 (4.41)	3.86	

[a] B3LYP/6-31G(d,p) values in the gas phase are given in parentheses.

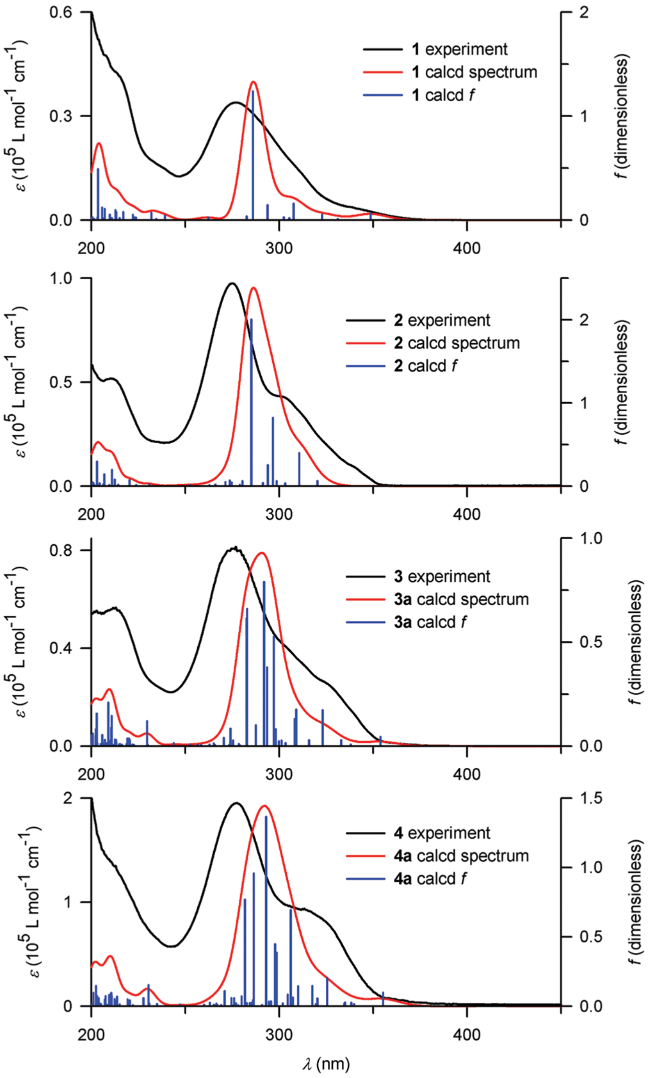

Figure 9. UV−vis electronic absorption spectra computed at the TD-B3LYP/6-31G(d,p) level with the IEF-PCM-UA0 solvent model for cyclohexane. Gaussian-function convolutions (fwhm = 0.1 eV) and vertical scaling are applied to match experimental spectra in cyclohexane. Oscillator strengths, *f*, for vertical transitions are shown as stick plots.

properties of **2** such as large E_g and fluorescence quantum yield of about 20% are most representative of parent hydroazaacenes with cross-conjugated π-systems (Figure 3). Electrochemically estimated HOMO energies of −4.8 eV for **2**−**4** suggest propensity for a facile one-electron oxidation and just sufficient environmental stability toward oxygen (O_2).

4. EXPERIMENTAL SECTION

NMR and IR Spectroscopy, Mass Spectrometry, and Computations. NMR spectra (^{1}H, 400, 500, and 600 MHz) were obtained using benzene-d_6, acetone-d_6, and chloroform-*d* ($CDCl_3$) as solvent. The 500 MHz instrument was equipped with a cryoprobe. The chemical shift references were as follows: (^{1}H) benzene-d_5, 7.15 ppm; (^{13}C) benzene-d_5, 128.39 ppm (benzene-d_6), (^{1}H) acetone-d_5, 2.05 ppm; (^{13}C) acetone-d_5, 29.92 ppm (acetone-d_6), (^{1}H) chloroform, 7.26 ppm; (^{13}C) $CDCl_3$, 77.0 ppm ($CDCl_3$). Natural abundance ^{1}H−^{15}N HSQC spectra were externally referenced to $^{15}N_2$-labeled urea (98+% ^{15}N, 0.7 mg in 0.4 mL of acetone-d_6). The reported ^{15}N chemical shifts were converted to the δ ^{15}N (nitromethane) = 0 ppm scale,[76] using the relation: δ ^{15}N (urea) = δ ^{15}N (nitromethane) + 304.7 ppm.[77]

IR spectra were obtained using an instrument equipped with an ATR sampling accessory. For HR-FABMS, 3-nitrobenzylalcohol (3-NBA) and 1-(2-nitrophenoxy)octane (*o*-nitrophenyl octyl ether = ONPOE) were used as matrices.

DFT and TD-DFT computations were carried out using an 8-CPU workstation running Gaussian 03 and/or Gaussian 09.[60] All optimized geometries had rms forces in Cartesian coordinates of about 1.3 × 10^{-6} a.u or less, except for hexaamine **4a**, for which the rms forces were 3.5 × 10^{-6} au. All reported computed structures are minima on the B3LYP/6-31G(d,p) gas phase potential energy surface, as determined by vibrational analyzes (Table S4, Supporting Information).

X-ray Crystallography. Crystals of **2** for X-ray studies were prepared by sublimation under high vacuum. Data collections were performed at the Advanced Photon Source, Argonne National Laboratory in Chicago, using synchrotron radiation (λ = 0.49595 Å). Final cell constants were calculated from the xyz centroids of strong reflections from the actual data collection after integration (SAINT);[78] intensity data were corrected for absorption (SADABS).[79] The space group *C*2 was determined based on intensity statistics and systematic absences. The structure was solved with direct methods using Sir2004[80] and refined with full-matrix least-squares/difference Fourier cycles using SHELXL-97.[81] All non-hydrogen atoms were refined with anisotropic displacement parameters. The hydrogen atoms were placed in ideal positions and refined as riding atoms with relative isotropic displacement parameters. Disorder was refined for both *tert*-butyl groups. Crystal and structure refinement data for **2** are in the Supporting Information and the accompanying file in CIF format.

UV−vis and Fluorescence Spectroscopy. UV−vis absorption and fluorescence spectra were obtained in cyclohexane. Fluorescence quantum yields (ϕ_f) were determined in reference to quinine sulfate solution in 0.5 N H_2SO_4 (ϕ_f = 0.546) at 297 K.

Electrochemistry. Cyclic voltammetry and square wave voltammetry data were obtained under argon atmosphere using a commercial potentiostat/galvanostat. About 1 mg of **1**−**4** was dissolved in the supporting electrolyte solution (2.4 mL), 0.1 M tetrabutylammonium hexafluorophosphate (n-Bu_4NPF_6) in anhydrous DCM, and then transferred to a custom-made cell equipped with quasi-reference (Ag wire), counter (Pt foil), and working (100 μm Pt-disk) electrodes. The redox potentials were referenced to SCE using an internal decamethylferrocene (−0.130 V vs SCE for $Cp^*_2Fe/Cp^*_2Fe^+$ in CH_2Cl_2).[73] For each compound, plots of peak current vs square root of scan rate (50−500 or 20−500 mV/s) in cyclic voltammetry were linear. A detailed description of the voltammetry may be found in the Supporting Information.

Synthesis. Standard techniques for synthesis under inert atmosphere (argon or nitrogen), using custom-made Schlenk glassware, custom-made double manifold high vacuum lines, and argon-filled Vacuum Atmospheres gloveboxes, were employed. Chromatographic separations were carried out using normal phase silica gel. For selected separations, chromatography was carried out at 0 °C and/or silica gel was deactivated by treatment with 2−5% of triethylamine in pentane or hexane.[58]

General Procedures for Pd-Catalyzed Aminations Leading to Bromoamines 6 and 11 (Partial Br→NH Exchange). 1,3-Dibromo-4,6-diisopropenyl-benzene (1.5−2.0 mmol), sodium *tert*-butoxide (1.5 equiv), $Pd(OAc)_2$ (5−10 mol %), and DPPF (15−17 mol %) were charged to a Schlenk vessel under N_2. 4-*tert*-Alkylaniline (0.6−1.3 equiv) in toluene (7.5 mL) was added, and the reaction mixture was stirred for 1−3 d at 90 °C. Then the mixture was filtered through a plug of silica gel with pentane/benzene 9:1, evaporated, and purified by column chromatography.

Preparation of Bromoamine **6**. According to the general procedure, 1,3-dibromo-4,6-diisopropenylbenzene (0.472 g, 1.49 mmol) and 4-*tert*-butylaniline (0.32 mL, 2.00 mmol) provided 0.288 g (55%) of **6** as a colorless oil in 50% yield after chromatography (deactivated silica gel, pentane/benzene, 96:4). ^{1}H NMR (400 MHz, acetone-d_6): δ 7.358 (s, 1H), 7.343 (d, *J* = 8.8 Hz, 2H), 7.077 (d, *J* = 8.4 Hz, 2H), 7.005 (s, 1H), ~6.58 (br. s, 1H), 5.262 (m, 1H), 5.192 (m, 1H), 5.072 (m, 1H), 4.911 (m, 1H), 2.069 (dd, J = 1.6, 0.8 Hz, 3H), 2.051 (dd, J = ∼1.5, ∼1 Hz, 3H), 1.302 (s, 9H). ^{13}C NMR (100 MHz, acetone-d_6): δ 146.3, 145.3, 143.9, 142.1, 141.3, 136.7, 133.5, 130.7, 127.0, 120.72, 120.67, 120.0, 117.2, 116.4, 34.8, 31.8, 24.1, 23.5. IR (ZnSe): 3414, 3073, 2964, 2909, 1590, 1514, 1371, 1323, 1258, 1191 cm^{-1}. HRMS (FAB): calcd for $[C_{22}H_{26}N^{79}Br]^{+\bullet}$ 383.1243, found 383.1259; calcd for $[C_{22}H_{26}N^{81}Br]^{+\bullet}$ 385.1223, found 385.1230.

Preparation of Bromoamine ***11***. According to the general procedure 1,3-dibromo-4,6-diisopropenylbenzene (1.15 g, 3.67 mmol, 1.85 equiv) and 4-*tert*-undecylaniline (**10**) (0.490 g, 1.98 mmol) provided 391 mg (41%) of **11** as light reddish brown liquid after chromatography (ethyl acetate/hexane gradient 1:20, 1:10, and 1:5). R_f = 0.41 (Et_2O/hexane, 1:20). ^{1}H NMR (400 MHz, acetone-d_6): δ 7.349 (s, 1H), 7.292 (d, J = 8.8 Hz, 2H), 7.076 (d, J = 8.8 Hz, 2H), 7.002 (s, 1H), 6.55 (br. s, 1H, NH), 5.25−5.28 (m, 1H), 5.18−5.20 (m, 1H), 5.06−5.08 (m, 1H), 2.070 (dd, J = 1.5, 1.0 Hz, 3H), 2.05−2.06 (m, 3H), 1.58−1.64 (m, 2H), 1.282 (s, 6H), 1.19−1.31 (m, 10H), 1.06−1.14 (m, 2H), 0.855 (t, J = 7.0 Hz, 3H). ^{13}C NMR (100 MHz, acetone-d_6): 146.3, 143.8, 142.0, 141.0, 136.5, 133.2, 130.6, 127.5, 120.7, 120.6, 119.9, 117.2, 116.4, 45.4, 37.8, 32.6, 31.1, 30.3, 30.1, 29.6, 25.5, 24.1, 23.6, 23.4, 14.5. IR (ZnSe): 3404 (m), 2957 (s), 2925 (s), 2853 (s), 1592 (s), 1555 (m), 1513 (s), 1489 (s), 1367 (m), 1314 (s), 897 (s), 826 (m) cm^{-1}. HRMS (EI): calcd for $[C_{29}H_{40}N^{79}Br]^{+\bullet}$ 481.2339, found 481.2334; calcd for $[C_{29}H_{40}N^{81}Br]^{+\bullet}$ 483.2318, found 483.2320.

General Procedures for Pd-Catalyzed Aminations Leading to Oligoamines 7, 8, 15, 16, and 17 (Complete Br→NH Exchange). Under nitrogen atmosphere, mixtures of bromo and amino components, palladium(II) acetate (2−30 mol %), and sodium *tert*-butoxide (1.5 equiv) were placed in a resealable Schlenk vessel and dissolved/suspended in dry degassed toluene (10 mL/mmol). A solution of tri-*tert*-butylphosphine in toluene (0.3 M, 6−90 mol %, 3 equiv for Pd) was added, the vessel was sealed, and the mixture was stirred for 8−72 h at 90−100 °C. The mixture was subsequently cooled to room temperature and diluted with benzene, washed with brine, and dried over Na_2SO_4. Chromatography on deactivated (3% Et_3N) silica gel delivered the respective products.

Preparation of Tetraamine ***7***. According to the general procedure, **6** (0.322 g, 0.83 mmol), 2,6-diaminotoluene (47.6 mg, 0.39 mmol), and $Pd(OAc)_2$ (2.6 mg, 3 mol %) were stirred for 8 h at 90 °C to provide 0.192 g (67%) of **7** as yellow powder after chromatography (pentane/benzene, 1:1). Mp: 83−87 °C. ^{1}H NMR (400 MHz, acetone-d_6): δ 7.198 (d, J = 8.8 Hz, 4H), 7.035 (t, J = 8.0 Hz, 1H), 6.973 (s, 2H), 6.936 (d, J = 8.8 Hz, 4H), 6.794, (d, J = 8.0 Hz, 2H), 6.776 (s, 2H), ∼6.4 (br. s, 2H), ∼6.1 (br. s, 2H), 5.228 (m, 2H), 5.167 (m, 2H), 5.083 (m, 2H), 5.013 (m, 2H), 2.121 (s, 3H), 2.073 (s, 6H), 2.039 (br. s, 6H), 1.219 (s, 18H). ^{13}C NMR (100 MHz, acetone-d_6): δ 144.84, 144.79, 143.62, 143.51, 142.6, 141.9, 140.8, 129.9, 127.2, 126.68, 126.63, 126.2, 122.3, 118.1, 115.81, 115.67, 115.60, 107.7, 34.6, 31.9, 24.23, 24.08, 12.4. IR (ZnSe): 3407, 3073, 2961, 1583, 1513, 1471, 1391, 1370, 1327, 1256, 1193 cm^{-1}. HRMS (FAB): calcd for $[C_{51}H_{60}N_4]^{+\bullet}$ 728.4812, found 728.4835.

Preparation of Tetraamine ***8***. According to the general procedure, **6** (85.9 mg, 0.223 mmol), *m*-phenylenediamine (11.8 mg, 0.109 mmol), and $Pd(OAc)_2$ (1.0 mg, 2 mol %) were stirred for 12 h at 90 °C to give 72.5 mg (93%) of **8** as yellow powder after chromatography (pentane/benzene, 7:3). Mp: 92−93 °C. ^{1}H NMR (400 MHz, acetone-d_6): δ 7.197 (s, 2H), 7.183 (d, J = 8.8 Hz, 4H), 7.048 (t, J = 8.0 Hz, 1H), 7.001 (s, 2H), 6.988 (d, J = 8.8 Hz, 4H), 6.904 (t, J = 2.2 Hz, 1H), 6.536 (dd, J = 2.2, 8.0 Hz, 2H), 6.489 (br. s, 2H), 6.351 (br. s, 2H), 5.195 (m, 2H), 5.171 (m, 2H), 5.032 (m, 4H), 2.063 (s, 6H), 2.029 (s, 6H), 1.205 (s, 18H). ^{13}C NMR (100 MHz, acetone-d_6): δ 146.5, 144.8, 144.7, 143.9, 141.9, 140.9, 130.5, 130.2, 127.5, 127.3, 126.8, 118.8, 115.8, 115.9, 115.7, 109.7, 109.0, 105.2, 34.6, 31.9, 24.1, 24.0. IR (ZnSe): 3414, 2964, 2860, 1590, 1513, 1391, 1370, 1323, 1257, 1191, 899 cm^{-1}. HRMS (FAB): calcd for $[C_{50}H_{58}N_4]^{+\bullet}$ 714.4656, found 714.4683.

Preparation of Tetraamine ***15***. According to the general procedure, **11** (0.425 g, 0.881 mmol), 2,6-diamino-4′-*tert*-butylbiphenyl (**14**) (96.4 mg, 0.401 mmol), and $Pd(OAc)_2$ (29.6 mg, 33 mol %) were stirred for 72 h at 97 °C to provide 0.261 g (62%) of **15** as light brown oil after chromatography (ethyl acetate/pentane 1:20). R_f: 0.34 (Et_2O/hexane, 1:20). ^{1}H NMR (400 MHz, acetone-d_6): δ 7.590 (d, J = 8.5 Hz, 2H), 7.254 (d, J = 8.8 Hz, 2H), 7.211 (s, 2H), 7.157 (d, J = 8.5 Hz, 2H), 7.128 (t, J = 8.2 Hz, 1H), 7.062 (d, J = 8.8 Hz, 2H), 6.909 (d, J = 8.2, 2H), 6.828 (s, 2H), 6.43 (br. s 2H, NH), 5.76 (br. s 2H, NH), 5.152 (m, 2H), 4.990 (m, 2H), 4.876 (m, 2H), 4.416 (m, 2H), 2.022 (m, 6H), 1.803 (m, 6H), 1.621 (m, 2H), 1.368 (s, 9H), 1.285 (s 12H), 1.07 − 1.26 (m, 28H), 0.820 (t, J = 6.8 Hz, 6 H). ^{13}C NMR (126 MHz, acetone-d_6): δ 152.1, 144.7, 142.4, 142.3, 141.0, 139.7, 132.7, 131.1, 129.6, 128.8, 127.7, 127.3, 126.3, 125.9, 122.2, 118.9, 115.66, 115.54, 109.9, 106.0, 45.5, 37.8, 35.3, 32.7, 31.7, 31.3, 30.4, 30.2, 29.7, 25.6, 24.4, 24.0, 23.4, 14.5. IR (ZnSe): 3676 (m), 2989 (s), 2972 (s), 2901 (s), 1582 (m), 1513 (m), 1466 (m), 1406 (m), 1394 (m), 1384 (m), 1254 (m), 1231 (m), 1076 (s), 1066 (s), 1057 (s), 897 (m) cm^{-1}. HRMS (FAB): calcd for $[C_{74}H_{99}N_4]^{+\bullet}$ 1042.7786, found 1042.7784.

Preparation of Triamine ***16***. According to the general procedure, bromoamine **11** (0.128 g, 0.279 mmol), 2,6-diamino-4′-*tert*-butylbiphenyl (**14**) (63.2 mg, 0.263 mmol), and $Pd(OAc)_2$ (6.0 mg, 12 mol %) were stirred for 72 h at 100 °C to provide 49.7 mg (34%) of tetraamine **15** and 69.0 mg (43%) of triamine **16** as light brown oil after chromatography (diethyl ether/pentane 1:8). R_f: 0.49 (Et_2O/hexane, 1:5). ^{1}H NMR (400 MHz, acetone-d_6): δ 7.557 (d, J = 8.5 Hz, 2H), 7.248 (d, J = 8.8 Hz, 2H), 7.241 (s, 1H), 7.172 (d, J = 8.5 Hz, 2H), 7.049 (d, J = 8.8 Hz, 2H), 6.985 (t, J = 8.0 Hz, 1H), 6.809 (s, 1H), 6.716 (dd, J = 8.0 Hz, 0.8 Hz, 1H), 6.396 (s, 1H), 6.384 (dd, J = 8.0 Hz, 0.8 Hz, 1H), 5.667 (s, 1H), 5.143 (m, 1H), 4.986 (m, 1H), 4.888 (m, 1H), 4.393 (m, 1H), 4.055 (s, 1H), 2.018 (m, 3H), 1.807 (m, 3H), 1.58−1.64 (m, 2H), 1.358 (s, 9H), 1.273 (s, 6H), 1.20−1.30 (m, 10H), 1.07−1.14 (m, 2H), 0.860 (t, J = 6.9 Hz, 3H). ^{13}C NMR (100 MHz, acetone-d_6): δ 151.4, 147.1, 144.7, 144.0, 142.29, 142.24, 141.7, 140.8, 140.4, 133.6, 131.1, 129.4, 129.0, 127.4, 127.3, 125.6, 125.4, 118.7, 118.1, 115.51, 115.45, 108.8, 107.5, 105.4, 45.4, 37.7, 35.2, 32.7, 31.7, 31.2, 30.4, 30.1, 29.6, 25.6, 24.5, 24.0, 23.4, 14.5. IR (ZnSe): 3395 (w), 2960 (m), 2923 (m), 2852 (m), 1608 (m), 1581 (s), 1513 (s), 1464 (s), 1254 (m), 898 (m), 835 (m), 729 (m) cm^{-1}. HRMS (FAB): calcd for $[C_{45}H_{59}N_3]^{+\bullet}$ 641.4704, found 641.4708.

Preparation of Hexaamine ***17***. According to the general procedure, triamine **16** (38.2 mg, 59.5 μmol), 1,3-dibromo-4,6-diisopropenylbenzene (30.0 μmol), and $Pd(OAc)_2$ (1.6 mg, 24 mol %) were stirred for 168 h at 90−100 °C to give 20.4 mg (48%) of hexaamine **17** as light brown oil after chromatography (Et_2O/pentane 1:15). R_f = 0.58 (ethyl acetate/hexane, 1:10). ^{1}H NMR (400 MHz, acetone-d_6): δ 7.574 (d, J = 8.3 Hz, 4H), 7.295 (s, 1H), 7.278 (d, J = 8.6 Hz, 4H), 7.252 (s, 2H), 7.218 (t, J = 8.0 Hz, 2H), 7.158 (d, J = 8.3 Hz, 4H), 7.088 (d, J = 8.6 Hz, 4H), 6.990 (d, J = 8.0 Hz, 2 H), 6.978 (d, J = 8.0 Hz, 2 H), 6.847 (s, 2H), 6.686 (s, 1H), 6.413 (s, 2H), 5.774 (s, 2H), 5.724 (s, 2H), 5.168 (m, 2H), 5.013 (m, 2H), 4.892 (m, 2H), 4.861 (m, 2H), 4.440 (m, 2H), 4.392 (m, 2H), 2.040 (m, 6H), 1.820 (m, 6H), 1.771 (m, 6H), 1.59−1.65 (m, 4H), 1.356 (s, 18H), 1.288 (s, 12H), 1.19−1.28 (m, 20H), 1.07−1.17 (m, 4H), 0.813 (t, J = 6.5 Hz, 6H). ^{13}C NMR (100 MHz, acetone-d_6): δ 152.1, 144.7, 144.10, 144.08, 142.6, 142.5, 142.4, 142.2, 141.1, 141.0, 139.8, 139.7, 132.8, 131.1, 129.6, 129.1, 128.9, 127.7, 127.4, 126.2, 125.9, 125.3, 122.5, 119.13, 119.06, 115.7, 115.55, 115.50, 110.4, 110.1, 45.5, 37.8, 35.1, 32.7, 31.7, 31.3, 30.4, 30.2, 25.7, 24.4, 24.3, 24.0, 23.4, 14.5. IR (ZnSe): 3676 (m), 2989 (s), 2901 (s), 1454 (m), 1405 (m), 1394 (m), 1383 (m), 1250 (m), 1241 (m), 1230 (m), 1066 (s), 1058 (s), 1028 (m), 878 (m) cm^{-1}. HRMS (ESI): calcd for $[C_{102}H_{128}N_6 + H]^+$ 1438.0273, found 1438.0276.

General Procedure for Friedel−Crafts Cyclizations Leading to Oligoamines 3, 4 and 5. Amine (approximately 0.05 mmol) was placed in a pear-shaped flask under nitrogen flow and a degassed mixture of 98% sulfuric and 85% phosphoric acids was added (1:1 v/v, 0.5 mL). The mixture was continuously agitated with a glass rod for 15 min at 60 °C, cooled in an ice bath, and transferred into an ice-cold 10% aqueous NaOH solution. The precipitate was carefully extracted with benzene. The combined extracts were dried over Na_2SO_4 and evaporated.

Preparation of Tetraamine ***3***. According to the general procedure, **15** (71.0 mg) provided 66.8 mg (94%) of tetraamine **3** as a white solid. Mp (under argon): 230−232 °C. ^{1}H NMR (500 MHz, acetone-d_6): δ 7.721 (d, J = 8.1 Hz, 2H), 7.622 (s, 2H), 7.501 (s, 1H), 7.417 (s, 2H), 7.369 (d, *J* = 8.1 Hz, 2H), 7.359 (d, *J* = 2.0 Hz, 2H), 6.996 (dd, *J* = 8.2, 2.0 Hz, 2H), 6.655 (d, *J* = 8.2 Hz, 2H), 6.063 (s, 2H), 5.899 (s, 2H), 1.617 (s, 12H), 1.57−1.61 (m, 4H), 1.588 (s, 12H), 1.467 (s, 9H), 1.282 (s, 12H), 1.16−1.26 (m, 20 H), 1.05−1.11 (m, 4H), 0.835 (t, *J* = 6.9 Hz, 6H). ^{13}C NMR (126 MHz, acetone-d_6): δ 152.0, 141.1, 138.7, 138.3, 137.6, 135.5, 132.1, 131.9, 129.3, 129.3, 127.9, 124.7, 123.6, 123.3, 122.5, 122.3, 122.2, 113.8, 110.9, 98.7, 45.4, 37.9, 36.82, 36.79, 35.4, 32.6, 31.98, 31.90, 31.87, 31.81, 31.1, 25.5, 23.4, 14.4. IR (ZnSe): 3412 (m), 2958 (s), 2926 (s), 2856 (s), 1630 (m), 1607 (s), 1501 (s), 1465 (s), 1419 (m), 1294 (s), 1181(m), 809 (m) cm^{-1}. HRMS (FAB): calcd for $[\mathrm{C}_{74}\mathrm{H}_{98}\mathrm{N}_4]^{+\bullet}$ 1042.7786, found 1042.7773, calcd for $[\mathrm{C}_{74}\mathrm{H}_{98}\mathrm{N}_4 + \mathrm{H}]^+$ 1043.7864, found 1043.7866.

*Preparation of Hexaamine **4**.* According to the general procedure, **16** (16.9 mg, 0.0117 mmol) provided 11.2 mg (66%) of hexaamine **4** as a white solid after chromatography on deactivated silicagel at 0 °C (ethyl acetate/benzene/pentane, 2:1:20). Mp (under argon): 272 °C dec. R_f = 0.31 (pentane/ethyl acetate, 12:1). ^{1}H NMR (500 MHz, acetone-d_6): δ 7.663 (d, *J* = 8.2 Hz, 4H), 7.635 (s, 2H), 7.484 (s, 2H), 7.417 (s, 1H), 7.404 (s, 2H), 7.351 (d, *J* = 2.3 Hz, 2H), 7.314 (d, *J* = 8.2 Hz, 4H), 6.992 (dd, *J* = 8.3, 2.3 Hz, 2H), 6.650 (d, *J* = 8.3 Hz, 2H), 6.088 (s, 2H), 5.981 (s, 2H), 5.868 (s, 2H), 5.646 (s, 1H), 1.605 (s, 12H), 1.597 (s, 12H), 1.57−1.60 (m, 4H), 1.555 (s, 12H), 1.425 (s, 18H), 1.17−1.31 (m, 20H), 1.256 (s, 12H), 1.04−1.10 (m, 4H), 0.829 (t, J = 6.9 Hz, 6H). ^{1}H NMR (600 MHz, benzene-d_6): δ 7.713 (s, 2H), 7.586 (s, 1H), 7.545 (d, *J* = 2.0 Hz, 2H), 7.513 (s, 2H), 7.477 (d, *J* = 8.3 Hz, 4H), 7.353 (d, *J* = 8.3 Hz, 4H), 7.211 (dd, *J* = 8.2, 2.0 Hz, 2H), 6.527 (d, *J* = 8.2 Hz, 2H), 5.788 (s, 2H), 5.660 (s, 2H), 5.182 (s, 2H), 4.792 (s, 2H), 4.187 (s, 1H), 1.852 (s, 12H), 1.837 (s, 12H), 1.69−1.73 (m, 4H), 1.700 (s, 12H), 1.404 (s, 12H), 1.303 (s, 18H), 1.19−1.30 (m, 24H), 0.878 (t, J = 7.0 Hz, 6H). ^{13}C NMR (151 MHz, benzene-d_6): δ 151.9, 141.8, 137.98, 137.83, 137.84, 137.7, 137.2, 135.7, 135.4, 133.0, 132.4, 129.8, 127.9, 124.6, 123.6, 123.05, 122.96, 122.85, 122.81, 122.76, 122.74, 122.5, 113.6, 110.5, 99.0, 98.6, 45.6, 38.0, 36.93, 36.90, 36.88, 36.2, 32.8, 32.6, 32.3, 31.9, 31.3, 30.3, 30.1, 30.0, 23.4, 25.7, 14.9. IR (ZnSe): 3673 (m), 2989 (s), 2972 (s), 2900 (s), 1405 (m), 1394 (m), 1383 (m), 1250 (m), 1241 (m), 1230 (m), 1076 (s), 1066 (s), 1058 (s), 1028 (m), 879 (m) cm^{-1}. HRMS (FAB): calcd for $[\mathrm{C}_{102}\mathrm{H}_{128}\mathrm{N}_6]^{+\bullet}$ 1437.0195, found 1437.0223; calcd for $[\mathrm{C}_{102}\mathrm{H}_{128}\mathrm{N}_6 + \mathrm{H}]^+$ 1438.0273, found 1438.0257.

*Preparation of Tetraamine **5**.* According to the general procedure **8** (17.6 mg, 0.0246 mmol) provided 3.9 mg of **5** (22%) as brown solid after PTLC (3% deactivated silica gel, benzene). Mp (under air): 200 °C dec. Mp (under argon): >320 °C dec, 350 °C (liquid). ^{1}H NMR (400 MHz, acetone-d_6): δ 7.781 (br. s, 1H, exch $\mathrm{D_2O}$), 7.762 (br. s, 1H, exch $\mathrm{D_2O}$), 7.694 (br. s, 1H, exch $\mathrm{D_2O}$), 7.439 (br. s, 3H), 7.408 (s, 1H), 7.107 (d, *J* = 8.4 Hz, 1H), 7.082 (dd, *J* = 2.0, 8.0 Hz, 1H), 7.069 (dd, *J* = 2.0, 8.0 Hz, 1H), 6.764 (br. s, 1H, exch $\mathrm{D_2O}$), 6.717 (d, *J* = 8.4 Hz, 1H), 6.685 (d, *J* = 8.4 Hz, 1H), 6.433 (s, 1H), 6.295 (d, *J* = 8.0 Hz, 1H), 6.084 (s, 1H), 1.930 (s, 6H), 1.595 (s, 6H), 1.584 (s, 6H), 1.504 (s, 6H), 1.297 (s, 18H). IR (ZnSe): 3406 (m), 2962 (s), 2924(s), 2856 (s), 1630 (m), 1608 (s), 1501 (s), 1462 (s), 1415 (m), 1302 (m) cm^{-1}. HRMS (ESI): calcd for $[\mathrm{C}_{50}\mathrm{H}_{58}\mathrm{N}_4]^{+\bullet}$ 714.4656, found 714.4683.

*Preparation of Tetraamine **2**.* Phosphoric acid (85%, 2.0 mL) was added to tetraamine **7** (83.0 mg, 0.113 mmol) under $\mathrm{N_2}$. After 6 h at 90 °C, the reaction mixture was poured into $\mathrm{H_2O}$. The precipitate was collected and dissolved in THF. The obtained red solution was poured into aqueous KOH (0.02 M) and MeOH, which gave a yellow precipitate that was triturated with MeOH and MeOH/KOH and dried under vacuum to give a yellow powder. Precipitation from THF and aqueous KOH gave tetraamine **2** as light brown solid (54.0 mg, 65%). Mp (under Ar): >430 °C dec, 448 °C (liquid). ^{1}H NMR (400 MHz, acetone-d_6,): δ ~7.71 (br s, 2H, exch $\mathrm{D_2O}$), 7.431 (d, *J* = 2.0 Hz, 2H), 7.406 (s, 2H), 7.345 (s, 1H), ~7.11 (br. s, 2H, exch $\mathrm{D_2O}$), 7.059 (dd, *J* = 2.0, 8.4 Hz, 2H), 6.676 (d, *J* = 8.4 Hz, 2H), 6.401 (s, 2H), 2.184 (s, 3H), 1.577 (s, 12H), 1.569 (s, 12H), 1.291 (s, 18H). IR (ZnSe): 3673 (m), 2989 (s), 2971 (s), 2901 (s), 1630 (w), 1613 (m), 1504 (m), 1491 (m), 1406 (m), 1394 (m), 1383 (m), 1250 (m), 1231 (m), 1066 (s), 1057 (s), 1028 (m) cm^{-1}. HRMS (FAB): calcd for $[\mathrm{C}_{51}\mathrm{H}_{60}\mathrm{N}_4]^{+\bullet}$ 728.4812, found 728.4807, calcd for $[\mathrm{C}_{51}\mathrm{H}_{60}\mathrm{N}_4 + \mathrm{H}]^+$ 729.4891, found 729.4872.

*4-Nitro-(1,1-dimethylnonyl)benzene (**9**).* A mixture of concentrated nitric acid (4.1 mL) and concentrated sulfuric acid (2.6 mL) was cooled to 5 °C and then added to 2-methyl-2-phenyldecane (4.19 g, 18.1 mmol) and stirred vigorously in an ice−water bath. The heterogeneous mixture was allowed to attain room temperature. After being stirred at room temperature for 16 h, the reaction mixture was poured onto ice, $\mathrm{Na_2CO_3}$ was added until the pH turned alkaline, and the mixture was extracted with hexane and dried over $\mathrm{Na_2SO_4}$. Column chromatography on silica gel with $\mathrm{CH_2Cl_2}$/hexane (1:20 to 1:13) gave **9** as light yellow liquid (3.61 g, 88%). R_f = 0.27 (benzene/hexane, 1:25). ^{1}H NMR (400 MHz, $\mathrm{CDCl_3}$): δ 8.151 (d, *J* = 8.9 Hz, 2H), 7.473 (d, J = 8.9 Hz, 2H), 1.60 − 1.65 (m, 2H), 1.328 (s, 6H), 1.15−1.29 (m, 10H), 0.96−1.04 (m, 2H), 0.853 (t, *J* = 7.0 Hz, 3H). ^{13}C NMR (100 MHz, $\mathrm{CDCl_3}$): δ 157.8, 145.9, 126.7, 123.2, 44.4, 38.5, 31.8, 30.2, 29.4, 29.2, 28.7, 24.6, 22.6, 14.0. IR (ZnSe): 2925 (m), 2854 (m), 1598 (m), 1516 (s), 1465 (m), 1340 (s), 1109 (m), 851 (s), 758 (m), 700 (s) cm^{-1}.

*4-(1,1-Dimethylnonyl)aniline (**10**).* 4-Nitro(1,1-dimethylnonyl)-benzene (**9**) (1.698 g, 6.12 mmol) and acetic acid (60 mL) were placed in a round-bottom flask equipped with a reflux condenser. Iron powder (325 mesh, 6.72 g, 121 mmol) was added, and the suspension was stirred vigorously at room temperature. (Initial raise in temperature was observed due to an exothermic reaction.) After 16 h, the mixture was evaporated and the residue was treated with powdered KOH, the product was taken up in benzene and filtered through a pad of Celite. Removal of solvents afforded 1.445 g (96%) of pure **10** as light orange liquid. ^{1}H NMR (400 MHz, $\mathrm{CDCl_3}$): δ 7.119 (d, *J* = 8.3 Hz, 2H), 6.646 (d, J = 8.3 Hz, 2H), 3.6 (br. 2H, $\mathrm{NH_2}$), 1.50−1.56 (m, 2H), 1.241 (s, 6H), 1.12−1.31 (m, 10H), 1.00−1.09 (m, 2H), 0.866 (t, *J* = 6.9 Hz, 3H). ^{13}C NMR (100 MHz, $\mathrm{CDCl_3}$): δ 143.5, 140.1, 126.6, 114.9, 44.7, 36.8, 31.9, 30.4, 29.5, 29.3, 29.1, 24.7, 22.6, 14.1. IR (ZnSe): 3360 (w), 2955 (m), 2926 (s), 2853 (m), 1621 (s), 1516 (s), 1466 (m), 1278 (m), 1189 (m), 912 (m), 825 (s), 736 (s) cm^{-1}. HRMS (CI): calcd for $[\mathrm{C}_{17}\mathrm{H}_{29}\mathrm{N}]^{+\bullet}$ 247.2295 found 247.2292, calcd for $[\mathrm{C}_{17}\mathrm{H}_{29}\mathrm{N} + \mathrm{H}]^+$ 248.2373 found 248.2388.

*4′-tert-Butyl-2,6-dibromobiphenyl (**12**).* 2-Iodo-1,3-dibromobenzene (2.10 g, 5.82 mmol), 4-*tert*-butylphenylboronic acid (1.16 g, 6.52 mmol, 1.12 equiv), and tetrakis(triphenylphosphino)palladium (0) (69.4 mg, 0.060 mmol, 1.0 mol %) were charged to a Schlenk vessel. Then, a mixture of degassed benzene (40 mL), ethanol (10 mL), and aqueous $\mathrm{Na_2CO_3}$ solution (2 M, 10 mL) was added. The mixture was stirred vigorously at 85−95 °C for 168 h. After attaining room temperature, the reaction mixture was extracted with benzene, washed with NaOH solution (10%), dried over $\mathrm{Na_2SO_4}$, and concentrated. Chromatography on silica gel with hexane gave 1.74 g (81%) of **12** as colorless oil. R_f = 0.58 (benzene/hexane, 1:25). ^{1}H NMR (400 MHz, $\mathrm{CDCl_3}$): δ 7.626 (d, *J* = 8.0 Hz, 2H), 7.465 (d, *J* = 8.1 Hz, 2H), 7.143 (d, J = 8.1 Hz, 2H) 7.050 (t, *J* = 8.0 Hz, 1H), 1.383 (s, 9H). ^{13}C NMR (100 MHz, $\mathrm{CDCl_3}$): δ 150.9, 143.1, 138.1, 131.8, 129.6, 128.7, 125.0, 124.8, 34.7, 31.4. IR (ZnSe): 3085 (w), 3052 (w), 2962 (m), 2905 (m), 2864 (m), 1546 (s), 1476 (m), 1461 (m), 1431 (s), 1420 (s), 1397 (m), 1362 (m), 1268 (m), 1188 (s), 1114 (m), 1026 (m), 832 (s), 771 (s), 717 (s) cm^{-1}. HRMS (EI): calcd for $[\mathrm{C}_{16}\mathrm{H}_{16}{}^{79}\mathrm{Br}_2]^{+\bullet}$ 365.9613, found 365.9610.

*2,6-Bis(N-benzylamino)-4′-tert-butylbiphenyl (**13**).* Dibromo compound **12** (0.743 g, 2.02 mmol) was evacuated in a Schlenk vessel. Then, in a glovebag, palladium(II) acetate (35.6 mg, 0.16 mmol, 7.9 mol %), BINAP (212.8 mg, 0.342 mmol 17 mol %), and sodium *tert*-butoxide (0.770 g, 8.02 mmol, 3.97 equiv) were added. Dry degassed toluene (33 mL) and benzylamine (8.8 mL, 81 mmol, 40 equiv) were added. The reaction mixture was stirred at 120 °C for 25 h. After attaining room temperature, the reaction mixture was diluted with ethyl acetate, washed with brine, dried over $\mathrm{Na_2SO_4}$, and concentrated. The residual benzylamine was removed in high vacuum. Flash chromatography on deactivated silica gel (4% $\mathrm{Et_3N}$) with ethyl acetate/benzene/hexane (5:2:100) afforded yellowish solid that was washed with pentane (2 × 0.6 mL) to give 0.686 g (81%) of pure **13** as a white crystalline solid. Mp: 130−133 °C. ^{1}H NMR (400 MHz,

$CDCl_3$): δ 7.574 (d, *J* = 8.3 Hz, 2H), 7.364 (d, *J* = 8.3 Hz, 2H), 7.22 − 7.38 (m, 10H), 7.035 (t, *J* = 8.2 Hz, 1H), 6.149 (d, *J* = 8.2 Hz, 2H), 4.330 (d, *J* = 5.9 Hz, 4H), 3.876 (t, *J* = 5.9 Hz, 2H, NH), 1.401 (s, 9H). ^{13}C NMR (100 MHz, $CDCl_3$): δ 150.7, 145.9, 140.1, 132.0, 130.9, 129.0, 128.4, 127.0, 126.8, 126.7, 112.3, 101.0, 47.9, 34.6, 31.3. IR (ZnSe): 3436 (m), 2963 (m), 2863 (m), 1580 (s), 1574 (s), 1495 (s), 1473 (s), 1453 (m), 1237 (m), 840 (m), 740 (s), 697 (s) cm^{-1}. HRMS (FAB): calcd for $[C_{30}H_{32}N_2]^{+\bullet}$ 420.2560, found 420.2559.

*2,6-Diamino-4′-tert-butylbiphenyl (**14**).* Diamine **13** (0.810 g, 1.92 mmol) was suspended in ethanol (80 mL) in a round-bottom flask equipped with a reflux condenser. A small amount of recrystallized ammonium formate (∼0.01 g) was added, followed by 10% palladium on charcoal (72 mg, 0.068 mmol, 3.5 mol %). The mixture was stirred under reflux, and recrystallized ammonium formate was added in portions (total 1.44 g, 22.9 mmol, 11.9 equiv) over 3 h. The reflux was continued for 46 h, and the mixture was cooled to room temperature, filtered through Celite, and concentrated. The residue was dissolved in ethyl acetate and washed with brine. The aqueous phase was extracted with ethyl acetate, and the combined organic extracts were dried over Na_2SO_4 and filtered. Evaporation afforded 0.442 g (96%) of pure **14** as a white solid. Mp: 179−180 °C. ^{1}H NMR (400 MHz, $CDCl_3$): δ 7.505 (d, *J* = 8.6 Hz, 2H), 7.286 (d, *J* = 8.6 Hz, 2H), 6.951 (t, *J* = 8.0 Hz, 1H), 6.233 (d, *J* = 8.0 Hz, 2H), 3.45 (br. 4H, NH_2), 1.359 (s, 9H). ^{1}H NMR (400 MHz, acetone-d_6): δ 7.544 (d, *J* = 8.6 Hz, 2H), 7.228 (d, *J* = 8.6 Hz, 2H), 6.784 (t, *J* = 7.9 Hz, 1H), 6.132 (d, *J* = 7.9 Hz, 2H), 3.87/3.84 (br. 4H, NH_2), 1.355 (s, 9H). ^{13}C NMR (100 MHz, acetone-d_6): δ 150.8, 146.68, 146.65, 134.5, 131.2, 129.2, 127.2, 105.4, 35.9, 31.7. IR (ZnSe): 3464 (m), 3373 (m), 2962 (m), 2949 (m), 1612 (s), 1598 (m), 1581 (m), 1464 (s), 1270 (m), 1114 (m), 1001 (m), 840 (s), 779 (s), 726 (s) cm^{-1}. HRMS (FAB): calcd for $[C_{16}H_{20}N_2]^{+\bullet}$ 240.621, found 240.1633.

■ ASSOCIATED CONTENT

Supporting Information

General procedures and materials, additional experimental details, X-ray crystallographic file for **2** (CIF), and complete ref 60. This material is available free of charge via the Internet at http://pubs.acs.org.

■ AUTHOR INFORMATION

Corresponding Author

*E-mail: arajca1@unl.edu.

Notes

§On leave from Wrocław University of Technology, Poland.

■ ACKNOWLEDGMENTS

We thank the National Science Foundation for support of this research through Grant Nos. CHE-0718117 and CHE-1012578. ChemMatCARS Sector 15 is principally supported by the National Science Foundation/Department of Energy under Grant No. NSF/CHE-0822838. Use of the Advanced Photon Source was supported by the U.S. Department of Energy, Office of Science, Office of Basic Energy Sciences, under Contract No. DE-AC02-06CH11357. We thank Bridget Foley for preliminary synthesis of derivatives of building block **14**.

■ REFERENCES

(1) Yu, L.; Chen, M.; Dalton, L. R. *Chem. Mater.* **1990**, *2*, 649−659.

(2) Kim, F. S.; Ren, G.; Jenekhe, S. A. *Chem. Mater.* **2011**, *23*, 682−732.

(3) (a) Usta, H.; Facchetti, A.; Marks, T. J. *Acc. Chem. Res.* **2011**, *44*, 501−510. (b) Facchetti, A. *Chem. Mater.* **2011**, *23*, 733−758.

(4) Dong, H.; Wang, C.; Hu, W. *Chem. Commun.* **2010**, *46*, 5211−5222.

(5) Fukazawa, A.; Yamaguchi, S. *Chem. Asian J.* **2009**, *4*, 1386−1400.

(6) Babel, A.; Jenekhe, S. A. *J. Am. Chem. Soc.* **2003**, *125*, 13656−13657.

(7) Morita, Y.; Suzuki, S.; Sato, K.; Takui, T. *Nature Chem.* **2011**, *3*, 197−204.

(8) (a) Steinberg, B. D.; Jackson, E. A.; Filatov, A. S.; Wakamiya, A.; Petrukhina, M. A.; Scott, L. T. *J. Am. Chem. Soc.* **2009**, *131*, 10537−10545. (b) Valenti, G.; Bruno, C.; Rapino, S.; Marcaccio, M.; Paolucci, F.; Jackson, E. A.; Scott, L. T. *J. Phys. Chem. C* **2010**, *114*, 19467−19472. (c) Fort, E. H.; Scott, L. T. *Angew. Chem., Int. Ed.* **2010**, *49*, 6626−6628.

(9) (a) Roberson, L. B.; Kowalik, J.; Tolbert, L. M.; Kloc, C.; Zeis, R.; Chi, X.; Fleming, R.; Wilkins, C. *J. Am. Chem. Soc.* **2005**, *127*, 3069−3075. (b) Northrop, B. H.; Norton, J. E.; Houk, K. N. *J. Am. Chem. Soc.* **2007**, *129*, 6536−6546.

(10) (a) Wu, J.; Fechtenkötter, A.; Gauss, J.; Watson, M. D.; Kastler, M.; Fechtenkötter, C.; Wagner, M.; Müllen, K. *J. Am. Chem. Soc.* **2004**, *126*, 11311−11321. (b) Watson, M. D.; Fechtenkötter, A.; Müllen, K. *Chem. Rev.* **2001**, *101*, 1267−1300.

(11) Li, Y.; Gao, J.; Di Motta, S.; Negri, F.; Wang, Z. *J. Am. Chem. Soc.* **2010**, *132*, 4208−4213.

(12) Yuan, Z.; Xiao, Y.; Qian, X. *Chem. Commun.* **2010**, *46*, 2772−2774.

(13) Screen, T. E. O.; Thorne, J. R. G.; Denning, R. G.; Bucknall, D. G.; Anderson, H. L. *J. Am. Chem. Soc.* **2002**, *124*, 9712−9713.

(14) She, C.; Lee, S. J.; McGarrah, J. E.; Vura-Weis, J.; Wasielewski, M. R.; Chen, H.; Schatz, G. C.; Ratner, M. A.; Hupp, J. T. *Chem. Commun.* **2010**, *46*, 547−549.

(15) Pramanik, A.; Kang, H. S. *J. Chem. Phys.* **2011**, *134*, 094702−1−6.

(16) Hartley, C. S.; Elliott, E. L.; Moore, J. S. *J. Am. Chem. Soc.* **2007**, *129*, 4512−4513.

(17) Spitler, E. L.; Johnson, C. A. II; Haley, M. M. *Chem. Rev.* **2006**, *106*, 5344−5386.

(18) Rajca, A.; Rajca, S.; Pink, M.; Miyasaka, M. *Synlett* **2007**, 1799−1822.

(19) (a) Miyasaka, M.; Rajca, A.; Pink, M.; Rajca, S. *J. Am. Chem. Soc.* **2005**, *127*, 13806−13807. (b) Miyasaka, M.; Pink, M.; Rajca, S.; Rajca, A. *Angew. Chem., Int. Ed.* **2009**, *48*, 5954−5957. (c) Rajca, A.; Miyasaka, M.; Pink, M.; Xiao, S.; Rajca, S.; Das, K.; Plessel, K. *J. Org. Chem.* **2009**, *74*, 7504−7513. (d) Zak, J. K.; Miyasaka, M.; Rajca, S.; Lapkowski, M.; Rajca, A. *J. Am. Chem. Soc.* **2010**, *132*, 3246−3247.

(20) (a) Rajca, A.; Safronov, A.; Rajca, S.; Schoemaker, R. *Angew. Chem., Int. Ed. Engl.* **1997**, *36*, 488−491. (b) Rajca, A.; Rajca, S. *Angew. Chem., Int. Ed.* **2010**, *49*, 672−674.

(21) (a) Rajca, A.; Safronov, A.; Rajca, S.; Ross, C. R. II; Stezowski, J. J. *J. Am. Chem. Soc.* **1996**, *118*, 7272−7279. (b) Hudspeth, M. A.; Whitman, B. W.; Barone, V.; Peralta, J. E. *ACS Nano* **2010**, *4*, 4565−4570.

(22) Bendikov, M.; Wudl, F. *Chem. Rev.* **2004**, *104*, 4891.

(23) (a) Anthony, J. E. *Chem. Rev.* **2006**, *106*, 5028−5048. (b) Anthony, J. E. *Angew. Chem., Int. Ed.* **2008**, *47*, 452−483. (c) Zade, S. S.; Bendikov, M. *Angew. Chem., Int. Ed.* **2010**, *49*, 4012−4015.

(24) Extended acenes have open-shell singlet ground states: Bendikov, M.; Houk, K. N.; Duong, H. M.; Starkey, K.; Carter, E. A.; Wudl, F. *J. Am. Chem. Soc.* **2004**, *126*, 7416−7417;Correction: *J. Am. Chem. Soc.* **2004**, *126*, 10493.

(25) Kaur, I.; Stein, N. N.; Kopreski, R. P.; Miller, G. P. *J. Am. Chem. Soc.* **2009**, *131*, 3424−3425.

(26) Tönshoff, C.; Bettinger, H. F. *Angew. Chem., Int. Ed.* **2010**, *49*, 4125−4128.

(27) (a) Purushothaman, B.; Parkin, S. R.; Anthony, J. E. *Org. Lett.* **2010**, *12*, 2060−2063. (b) Griffith, O. L.; Anthony, J. E.; Jones, A. G.; Lichtenberger, D. L. *J. Am. Chem. Soc.* **2010**, *132*, 580−586.

(28) Dihydrodiazaacene: Wu, J. I.; Wannere, C. S.; Mo, Y.; Schleyer, P. v. R.; Bunz, U. H. F. *J. Org. Chem.* **2009**, *74*, 4343−4349.

(29) (a) Richards, G. J.; Hill, J. P.; Subbaiyan, N. K.; D'Souza, F.; Karr, P. A.; Elsegood, M. R. J.; Teat, S. J.; Mori, T.; Ariga, K. *J. Org. Chem.* **2009**, *74*, 8914−8923. (b) Tverskoy, O.; Rominger, F.; Peters, A.; Himmel, H.-J.; Bunz, U. H. F. *Angew. Chem., Int. Ed.*

2011, *50*, 3557–3560. (c) Gawrys, P.; Marszalek, T.; Bartnik, E.; Kucinska, M.; Ulanski, J.; Zagorska, M. *Org. Lett.* **2011**, *13*, 6090–6093.

(30) (a) Kummer, F.; Zimmermann, H. *Ber. Bunsen Ges. Phys. Chem.* **1967**, *71*, 1119–1127. (b) Miao, S.; Appleton, A. L.; Berger, N.; Barlow, S.; Marder, S. R.; Hardcastle, K. I.; Bunz, U. H. F. *Chem.—Eur. J.* **2009**, *15*, 4990–4993.

(31) Winkler, M.; Houk, K. N. *J. Am. Chem. Soc.* **2007**, *129*, 1805–1815.

(32) Appleton, A. L.; Brombosz, S. M.; Barlow, S.; Sears, J. S.; Bredas, J.-L.; Marder, S. R.; Bunz, U. H. F. *Nature Commun.* **2010**, *1*, 91.

(33) (a) Shiraishi, K.; Rajca, A.; Pink, M.; Rajca, S. *J. Am. Chem. Soc.* **2005**, *127*, 9312–9313. (b) Rajca, A.; Shiraishi, K.; Rajca, S. *Chem. Commun.* **2009**, 4372–4374. (c) Rajca, A.; Shiraishi, K.; Boratynski, P. J.; Pink, M.; Miyasaka, M.; Rajca, S. *J. Org. Chem.* **2011**, *76*, 8447–8457.

(34) Rajca, A.; Shiraishi, K.; Pink, M.; Rajca, S. *J. Am. Chem. Soc.* **2007**, *129*, 7232–7233.

(35) Boratyński, P. J.; Pink, M.; Rajca, S.; Rajca, A. *Angew. Chem., Int. Ed.* **2010**, *49*, 5459–5462.

(36) Triarylmethyl diradical, a derivative of pentacene: Rajca, A.; Utamapanya, S. *J. Org. Chem.* **1992**, *57*, 1760–1767.

(37) Oligo(*m*-aniline)s and nitroxide radicals with macrocyclic connectivity: (a) Vale, M.; Pink, M.; Rajca, S.; Rajca, A. *J. Org. Chem.* **2008**, *73*, 27–35. (b) Rajca, A.; Vale, M.; Rajca, S. *J. Am. Chem. Soc.* **2008**, *130*, 9099–9105.

(38) (a) Rajca, A.; Rajca, S.; Padmakumar, R. *Angew. Chem., Int. Ed. Engl.* **1994**, *33*, 2091–2093. (b) Rajca, A.; Lu, K.; Rajca, S. *J. Am. Chem. Soc.* **1997**, *119*, 10335–10345. (c) Rajca, A.; Wongsriratanakul, J.; Rajca, S.; Cerny, R. L. *Chem.–Eur. J.* **2004**, *10*, 3144–3157.

(39) (a) Ratera, I.; Veciana, J. *Chem. Soc. Rev.* **2012**, *41*, 303–349. (b) Lahti, P. M. *Adv. Phys. Org. Chem.* **2011**, *45*, 93–169. (c) Shishlov, N. M. *Russ. Chem. Rev.* **2006**, *75*, 863–884. (d) Rajca, A. *Adv. Phys. Org. Chem.* **2005**, *40*, 153–199. (e) Rajca, A. *Chem.—Eur. J.* **2002**, *8*, 4834–4841. (f) Rajca, A. *Chem. Rev.* **1994**, *94*, 871–893.

(40) (a) Fukuzaki, E.; Nishide, H. *J. Am. Chem. Soc.* **2006**, *128*, 996–1001. (b) Trinquier, G.; Suaud, N.; Malrieu, J.-P. *Chem.–Eur. J.* **2010**, *16*, 8762–8772. (c) Perrotta, R. R.; Winter, A. H.; Coldren, W. H.; Falvey, D. E. *J. Am. Chem. Soc.* **2011**, *133*, 15553–15558.

(41) (a) Rajca, S.; Rajca, A.; Wongsriratanakul, J.; Butler, P.; Choi, S. *J. Am. Chem. Soc.* **2004**, *126*, 6972–6986. (b) Rajca, A.; Wongsriratanakul, J.; Rajca, S. *J. Am. Chem. Soc.* **2004**, *126*, 6608–6626. (c) Rajca, A.; Shiraishi, K.; Vale, M.; Han, H.; Rajca, S. *J. Am. Chem. Soc.* **2005**, *127*, 9014–9020. (d) Rajca, A.; Takahashi, M.; Pink, M.; Spagnol, G.; Rajca, S. *J. Am. Chem. Soc.* **2007**, *129*, 10159–10170. (e) Rajca, A.; Olankitwanit, A.; Rajca, S. *J. Am. Chem. Soc.* **2011**, *133*, 4750–4753.

(42) (a) Rajca, A.; Wongsriratanakul, J.; Rajca, S. *Science* **2001**, *294*, 1503–1505. (b) Rajca, A.; Rajca, S.; Wongsriratanakul, J. *J. Am. Chem. Soc.* **1999**, *121*, 6308–6309.

(43) (a) Agou, T.; Kobayashi, J.; Kawashima, T. *Chem. Commun.* **2007**, 3204–3206. (b) Agou, T.; Kobayashi, J.; Kawashima, T. *Org. Lett.* **2006**, *8*, 2241–2244.

(44) Okamoto, T.; Kozaki, M.; Doe, M.; Uchida, M.; Wang, G.; Okada, K. *Chem. Mater.* **2005**, *17*, 5504–5511.

(45) (a) Wakim, S.; Bouchard, J.; Blouin, N.; Michaud, A.; Leclerc, M. *Org. Lett.* **2004**, *6*, 3413–3416. (b) Wakim, S.; Leclerc, M. *Synlett* **2005**, 1223–1234.

(46) Boudreault, P.-L. T.; Wakim, S.; Blouin, N.; Simard, M.; Tessier, C.; Tao, Y.; Leclerc, M. *J. Am. Chem. Soc.* **2007**, *129*, 9125–9136.

(47) Cross-conjugated poly(acene) precursors: Wang, H.; Schaffner-Hamann, C.; Marchioni, F.; Wudl, F. *Adv. Mater.* **2007**, *19*, 558–560.

(48) Gholami, M.; Tykwinski, R. R. *Chem. Rev.* **2006**, *106*, 4997–5027.

(49) Tian, Y.-H.; Park, G.; Kertesz, M. *Chem. Mater.* **2008**, *20*, 3266–3277.

(50) Cross-conjugation in electron transfer in molecular junctions: (a) Mayor, M.; Weber, H. B.; Reichert, J.; Elbing, M.; von Hänisch, C.; Beckmann, D.; Fischer, M. *Angew. Chem., Int. Ed.* **2003**, *42*, 5834–5838. (b) Solomon, G. C.; Herrmann, C.; Hansen, T.; Mujica, V.; Ratner, M. A. *Nature Chem.* **2010**, *2*, 223–228.

(51) (a) Slepkov, A. D.; Hegmann, F. A.; Zhao, Y.; Tykwinski, R. R.; Kamada, K. *J. Chem. Phys.* **2002**, *116*, 3834–3840. (b) Zucchero, A. J.; McGrier, P. L.; Bunz, U. H. F. *Acc. Chem. Res.* **2010**, *43*, 397–408.

(52) (a) Driver, M. S.; Hartwig, J. F. *J. Am. Chem. Soc.* **1996**, *118*, 7217–7218. (b) Hauck, S. I.; Lakshmi, K. V.; Hartwig, J. F. *Org. Lett.* **1999**, *1*, 2057–2060.

(53) (a) Hartwig, J. F.; Kawatsura, M.; Hauck, S. I.; Shaughnessy, K. H.; Alcazar-Roman, L. M. *J. Org. Chem.* **1999**, *64*, 5575–5580. (b) Nishiyama, M.; Yamamoto, T.; Koie, Y. *Tetrahedron Lett.* **1998**, *39*, 617–620.

(54) Fleckenstein, C. A.; Plenio, H. *Chem. Soc. Rev.* **2010**, *39*, 694–711.

(55) (a) Hellwinkel, D.; Schmidt, W. *Chem. Ber.* **1980**, *113*, 358–384. (b) Fox, J. L.; Chen, C. H.; Stenberg, J. F. *Org. Prep. Proc. Int.* **1985**, *17*, 169–173.

(56) In one reaction of **8** in phosphoric/sulfuric acid mixture, a trace amount of impure byproduct had the ^{1}H NMR spectrum that could correspond to a constitutional isomer of **5** with collinearly fused rings.

(57) Leroux, F.; Schlosser, M. *Angew. Chem., Int. Ed.* **2002**, *41*, 4272–4274.

(58) Spagnol, G.; Rajca, A.; Rajca, S. *J. Org. Chem.* **2007**, *72*, 1867–1869.

(59) Growth of high quality crystals of **3** and **4** was not successful. For tetraamine **3**, the best X-ray synchrotron data set was of low quality and had diffraction terminating at resolution of about 1 Å, most likely due to highly disordered side chains in the structure. A solution and limited refinement (R1 = 0.1496, wR2 = 0.3749 for the observed data) supports the atomic connectivity of the "tetraazanonacene" moiety (Figure S4, Supporting Information). The disorder of the side chains correlated. Weak and limited data do not allow for a full refinement of the structure.

(60) Frisch, M. J. et al. *Gaussian 03, Revision E.01*, Gaussian, Wallingford, CT, 2004. Frisch, M. J. et al. *Gaussian 09, Revision A.01*, Gaussian, Wallingford, CT, 2009.

(61) Jain, R.; Bally, T.; Rablen, P. R. *J. Org. Chem.* **2009**, *74*, 4017–4023.

(62) Saielli, G.; Nicolaou, K. C.; Ortiz, A.; Zhang, H.; Bagno, A. *J. Am. Chem. Soc.* **2011**, *133*, 6072–6077.

(63) Barone, G.; Gomez-Paloma, L.; Duca, D.; Silvestri, A.; Riccio, R.; Bifulco, G. *Chem.–Eur. J.* **2002**, *8*, 3233–3239.

(64) Tomasi, J.; Mennucci, B.; Cammi, R. *Chem. Rev.* **2005**, *105*, 2999–3094.

(65) Foley, M. J.; Singer, L. A. *J. Phys. Chem.* **1994**, *98*, 6430–6435.

(66) Experimental 0–0 excitation energies to S_1 for acenes (in eV): 4.77 (benzene in hexane), 4.00 (naphthalene in hexane), 3.31 (anthracene in hexane), 2.63 (tetracene in heptane), and 2.12 (pentacene in benzene): Birk, J. B. *Photophysics of Aromatic Molecules*; Wiley: New York, 1970; pp 44–83.

(67) (a) Utamapanya, S.; Rajca, A. *J. Am. Chem. Soc.* **1991**, *113*, 9242–9251. (b) Rajca, S.; Rajca, A. *J. Am. Chem. Soc.* **1995**, *117*, 9172–9179. (c) Hankache, J.; Wenger, O. S. *Chem. Rev.* **2011**, *111*, 5138–5178.

(68) De Leeuw, D. M.; Simenon, M. M. J.; Brown, A. R.; Einerhand, R. E. F. *Synth. Met.* **1997**, *87*, 53–59.

(69) Agrawal, A. K.; Jenekhe, S. A. *Chem. Mater.* **1996**, *8*, 579–589.

(70) Li, Y.; Cao, Y.; Gao, J.; Wang, D.; Yu, G.; Heeger, A. J. *Synth. Met.* **1999**, *99*, 243–248.

(71) (a) Raimundo, J. M.; Blanchard; Hugues Brisset, H.; Akoudad, S.; Roncali, J. *Chem. Commun.* **2000**, 939–940. (b) Roncali, J. *Macromol. Rapid Commun.* **2007**, *28*, 1761–1775.

(72) The −1.8 V to +1.7 V working potential window for dichloromethane when using tetrabutylammonium perchlorate and Pt working electrode was reported: Kadish, K. M.; Anderson, J. E. *Pure Appl. Chem.* **1987**, *59*, 703–714.

(73) Gennett, T.; Milner, D. F.; Weaver, M. J. *J. Phys. Chem.* **1985**, *89*, 2787–2794.

(74) Gierschner, J.; Cornil, J.; Egelhaaf, H.-J. *Adv. Mater.* **2007**, *19*, 173−191.

(75) Risko, C.; McGehee, M. D.; Bredas, J. L. *Chem. Sci.* **2011**, *2*, 1200−1218.

(76) Harris, R. K.; Becker, E. D.; de Menez, S. M. C.; Goodfellow, R.; Granger, P. *Pure Appl. Chem.* **2001**, *73*, 1795−1818.

(77) Wishart, D. S.; Bigam, C. G.; Yao, J.; Abildgaard, F.; Dyson, H. J.; Oldfield, E.; Markley, J. L.; Sykes, B. D. *J. Biomolecular NMR* **1995**, *6*, 135−140.

(78) *SAINT*, Bruker Analytical X-Ray Systems, Madison, WI, current version.

(79) Blessing, R. *Acta Crystallogr. A* **1995**, *51*, 33−38.

(80) Burla, M. C.; Caliandro, R.; Carnalli, M.; Carrozzini, B.; Cascarano, G. L.; De Caro, L.; Giacovazzo, C.; Polidori, G.; Sagna, R. *Sir2004, A Program for Automatic Solution and Refinement of Crystal Structure*, Version 1.0, 2004.

(81) (a) *SHELXTL-Plus V5.10*, Bruker Analytical X-Ray Systems, Madison, WI. (b) Sheldrick, G. M. *Acta Crystallogr. A* **2008**, *64*, 112−122.